Electronic Supplementary Material (ESI) for Green Chemistry.

Supporting Information

Stable and Reusable Nanoscale Fe_2O_3-catalyzed Aerobic Oxidation Process for Selective Synthesis of Nitriles and Primary Amides

Kathiravan Murugesan, Thirusangumurugan Senthamarai, Manzar Sohail, Muhammad Sharif, Narayana V. Kalevaru, and Rajenahally V. Jagadeesh*

Leibniz-Institut für Katalyse e. V. an der Universität Rostock, Albert-Einstein-Str. 29a, 18059 Rostock, Germany.

*Corresponding author: E-mail: Jagadeesh.Rajenahally@catalysis.de

Table of Contents:

S1. Materials and methods

Aldehydes, iron acetate, aqueous ammonia (320145 ACS reagent, 28.0-30.0% NH_3 basis, Sigma-Aldrich), 1,10-phenanthroline and other chemicals were obtained from various chemical companies. Carbon powder, VULCAN® XC72R with Code XVC72R and CAS No. 1333-86-4 was obtained from Cabot Corporation Prod. The pyrolysis experiments were carried out in Nytech-Qex oven.

TEM measurements were performed at 200 kV with an aberration-corrected JEM-ARM200F (JEOL, Corrector: CEOS). The microscope is equipped with a JED-2300 (JEOL) energy-dispersive x-ray-spectrometer (EDXS) for chemical analysis. The samples were deposited without any pre-treatment on a holey carbon supported Cu-grid (mesh 300) and transferred to the microscope. The High-Angle Annular Dark Field (HAADF) and Annular Bright Field (ABF) images were recorded with a spot size of approximately 0.1nm, a probe current of 120 pA and a convergence angle of 30-36°. The collection semi-angles for HAADF and ABF were 70-170 mrad and 11-22 mrad, respectively.

XPS data was obtained with a VG ESCALAB220iXL (ThermoScientific) with monochromatic Al Kα (1486.6 eV) radiation. The electron binding energies E_B were obtained without charge compensation. For quantitative analysis the peaks were deconvoluted with Gaussian-Lorentzian curves, the peak areas were divided by a sensitivity factor obtained from the element specific Scofield factor and the transmission function of the spectrometer.

EPR spectra in X-band were recorded on a Bruker EMX CW-micro spectrometer equipped with an ER 4119HS-WI high-sensitivity cavity and a variable temperature control unit using the following parameters: microwave power = 6.64 mW, modulation frequency = 100 kHz, modulation amplitude = 1 G.

Mössbauer spectra were obtained at 300 K and 77 K by a Mössbauer spectrometer from Wissel GmbH equipped with a ^{57}Co source. Isomer shifts are given relative to α-Fe at room temperature. The spectra were analyzed by least-square fits using Lorentzian line shapes.

GC conversions and yields were determined by GC-FID, HP6890 with FID detector, column HP530 m x 250 mm x 0.25 µm. NMR data were recorded on a Bruker ARX 300 and Bruker ARX 400 spectrometers.

S2. Procedure for the reparation of Fe_2O_3-N/C (Fe-Phen/C-800) catalyst (1 g) [2a]

Apropriate amounts of $Fe(OAc)_2$ and 1,10-phenanthroline corresponds to 3 wt% of Fe in 1:3 molar ratio of Fe to phenathroline were stirred in ethanol for 30 minutes at room temperature. Then, carbon powder (VULCAN® XC72R, Cabot Corperation Prod. Code XVC72R; CAS No. 1333-86-4) was added and the whole reaction mixture was stirred at 60 °C for 12-15 hours. The reaction mixture was cooled to room temperature and the ethanol was removed in vacuo. The solid material obtained was dried at 60 °C for 12 hours, after which it was grinded to a fine

powder. Then, the powdered material was pyrolyzed at 800 °C for 2 hours under an argon atmosphere and cooled to room temperature.

Elemental analysis of Fe2O3-N/C (pyrolyzed Fe-phen/C at 800 °C) (Wt%): C = 91.1, H = 0.19, N = 2.69, Fe = 2.95

S3. General procedure for the preparation of nitriles

The 8 mL oven dried glass vial was charged with magnetic stir bar and 0.5 mmol corresponding aldehyde and then 2 mL t-amyl alcohol was added. Next, 30 mg Fe_2O_3-N/C (Fe-Phen/C-800) catalyst (3 mol% Fe) was added followed the by the addition of 200-300 µL aq. NH_3 (28-30% NH_3 basis). The glass vial was fitted with septum and screw cap. Then 1 bar O_2 containing balloon was connected to the reaction vial though needle and reaction was allowed to procced for 24 hrs at 40 °C with stirring. After completion of the reaction, the reaction vial was cooled to room temperature and O_2 was discharged. Then, catalyst was filtered off, washed with ethyl acetate. The solvent from the filtrate containing the reaction product was removed in vacuo and corresponding nitrile was purified by column chromatography. In case of yields determined by GC, 100 µL n-hexadecane was added to the reaction vial containing products and diluted with ethyl acetate. Then, filtered through plug of silica and filtrate contain products was subjected GC analysis. Conversion and yields were determined by GC-FID (HP6890 with FID detector, column HP530 m x 250 mm x 0.25 µm) and compared with authentic samples. All products were analyzed by GC, GC-MS and NMR analysis.

S4. General procedure for the preparation of amides

A magnetic stirring bar and the corresponding aldehyde were transferred to 8 mL glass vial and then the 3 mL H_2O was added. Next, 50 mg Fe_2O_3-N/C (Fe-Phen/C-800) catalyst (5 mol% Fe) was added followed by the addition of 100 µL aq. NH_3 NH_3. Then, the vial was fitted with septum, cap and needle. The reaction vials (8 vials) were placed into a 300 mL autoclave (PARR Instrument Company) and then autoclave was pressurized with 10 bar of air. The autoclave was placed into an aluminium block and the temperature of the aluminium block was set to measure 120 °C inside the autoclave and reactions were allowed to progress under stirred condition for required time at 120 °C. In this set-up the temperature of the aluminium block was set more than 120 °C (130-140 °C) in ordered to attain exactly 120 °C inside the autoclave). After completion of the reactions, remaining air was discharged and the samples were removed from the autoclave. Then, catalyst was filtered off, washed with methanol. The solvent from the filtrate containing the reaction product was removed in vacuo and the corresponding amide was purified by column chromatography. All products were analyzed by GC-MS and NMR analysis.

S5. Procedure for the gram scale reactions

Under procedure mentioned in sections S4 with the condition, 2-5 g aldehyde, corresponds to 3 mol% Fe, 200 µL Aq. NH_3 for every 0.5 mmol substrate, 40 °C, 10-50 mL t-amyl alcohol, 24-30 h.

After completion of the reaction, the autoclave was cooled to room temperature and remaining air was discharged. The catalyst from the reaction mixture was filtered off and washed with ethyl acetate. The solvent from the filtrate containing reaction products was removed in vacuo. The corresponding nitrile was purified by column chromatography (silica; n-hexane-ethyl acetate mixture). All products were analyzed by GC-MS and NMR analysis.

S6. Procedure for catalyst recycling

The recycling of the catalyst system was carried out for the synthesis of benzonitrile under the same procedure given in the section S4 under reaction conditions: 1 mmol benzalydehyde, 60 mg Fe_2O_3-N/C (Fe-Phen/C-800) (3% Fe), 400 µL aq. NH_3, 1 bar O_2, 4mL t-amyl alcohol, 40 ^oC, 24 hrs, yields were determined by GC using 100 µL n-hexadecane standard. In each run, after the reaction the catalyst was separated by centrifugation, washed thoroughly with ethyl acetate and dried by vacuum. Then, the dried catalyst was used further, without any purification or re-activation.

S7. TEM measurements and data of Fe_2O_3-N/C (Fe-Phen/C-800) catalyst

TEM investigation of Fe-Phen/C-800 material (Fig. S1) was characterized by the formationFe_2O_3 particles of different size. Most of the oxide particles have a size between 20 and 80 nm, but occur always together with smaller ones of 2-5 nm size. Interestingly, these particles, including the small ones, are surrounded by a shell of a few graphene layers (best visible in the ABF image; Fig. S; left). The oxidic nature of the particles has been confirmed by Mössbauer, XPS and EPR results discussed below.

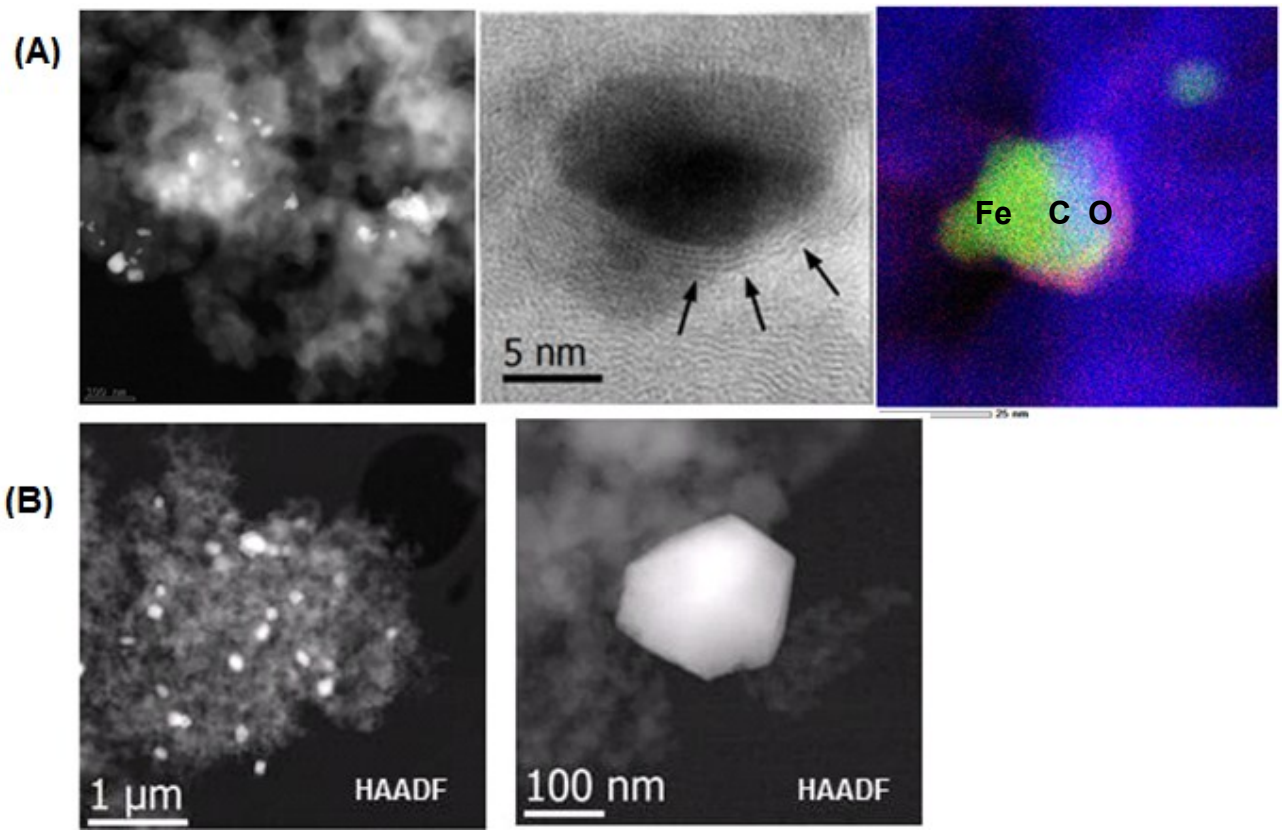

Fig. S1. TEM images of **(A):** Fe_2O_3-N/C (Fe-Phen/C-800)-catalyst: Right=HAADF image showing the distribution Fe_2O_3-particles; Middle= image showing Fe_2O_3-particle surrounded by nitrogen doped graphene layers; Right: EDXS map : iron = green, oxygen = red, carbon = blue. **(B):** $Fe(OAc)_2$/C-800 material, in which there is o formation of nitrogen doped graphene layers.

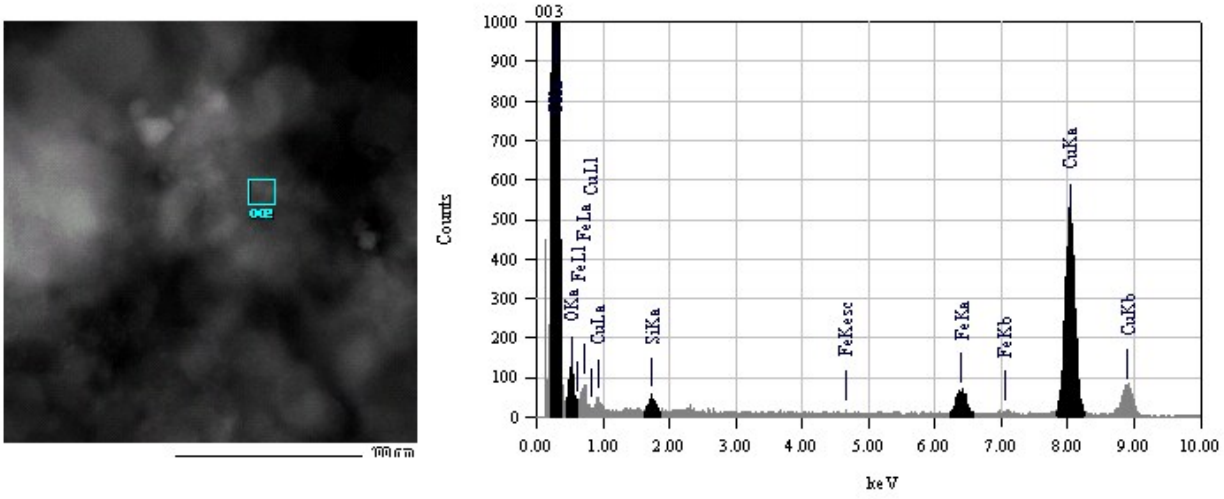

Fig. S2. EDX analysis of the Fe_2O_3 particles

S8. XPS mesurments and data of of Fe_2O_3-N/C (Fe-Phen/C-800) catalyst

XPS studies of Fe_2O_3-N/C (Fe-Phen/C-800) catalyst have been revealed that (Fig. S3) there are three N1s peaks occur at 398.3 eV, 399.3 eV and 401.0 eV. The first two peaks are assigned to pyridinic nitrogen and Fe-N centers, respectively [1]. A similar shift and even a splitting of the N1s peak was observed for 2H-tetraphenylporphyrin monolayers in contact with deposited Fe atoms on top. It was assigned to a so-called distorted FeN_4-center, [2] in which the Fe-N distances are slightly different, thus, giving rise to the peak splitting. It is probable that similar FeN_x-centers are formed with progressing pyrolysis on the surface of the emerging iron oxide particles. The fact that no splitting of the peak at 399.3 eV is observed may be due to a distribution of Fe-N distances which just contributes to the line width. The third N1s peak observed can be assigned to nitrogen in a graphite-like structure. [1] This suggests that N is incorporated into the support lattice.

The XPS for Fe2P electrons, two peaks corresponding to Fe species in the near-surface region were observed. The first one (major) appeared at 712.4 eV and the second one (minor) at 709.9 eV. The first peak is due to the presence of Fe^{+3} species (more likely Fe_2O_3) while the second one is assigned to Fe^{+2} species. Fe^{+2} species are in minor proportion compared to Fe^{+3}. Literature survey[3] reveals that the B.E. value of Fe 2p3/2 higher than 710.2 eV can be assigned to Fe^{3+} and the peak at 709.9 eV can be attributed to the presence of Fe^{+2} species.[4] Based on these results, in Fe-Phen/C-800 catalyst, both Fe^{+3} (major) and Fe^{+2} (minor) species are presented on the surface of the material. However, the bulk composition is somewhat different from the surface composition. In the bulk, we could see the presence of mainly the Fe^{+3} species (in the form of Fe_2O_3). The presence of Fe2O3 as particles has been confirmed by EPR analysis Mössbauer spectral analysis as follows.

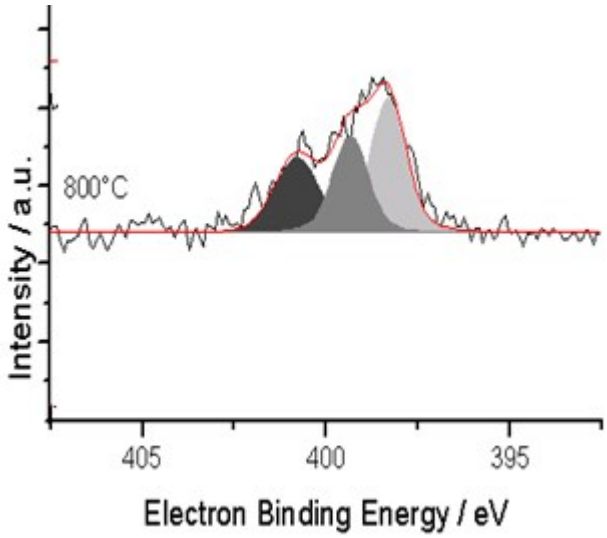

Fig. S3 A. XP spectra of the N1s electrons for the Fe_2O_3-N/C (Fe-Phen/C-800) catalyst

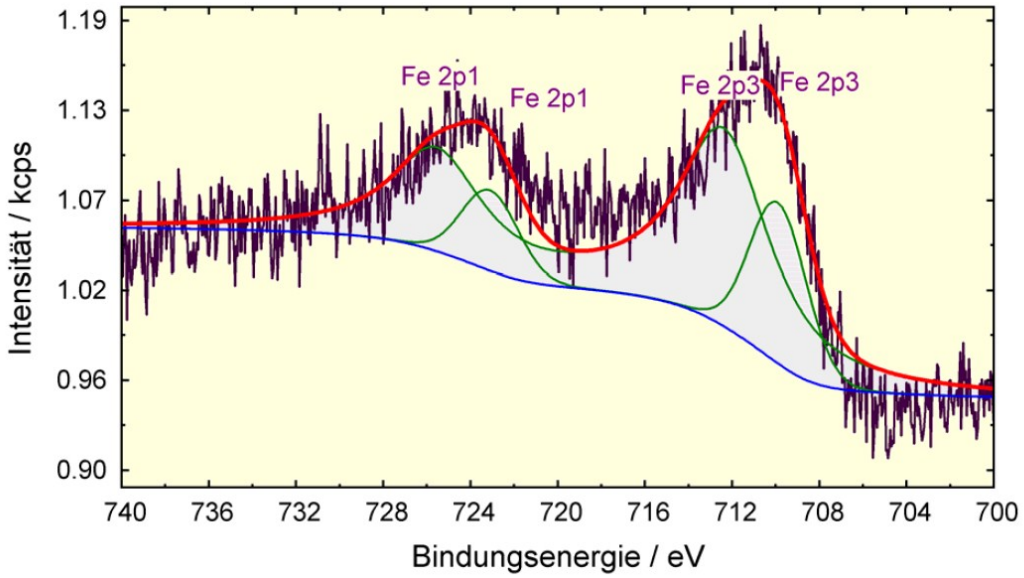

Fig. S3B. XP spectra of the Fe2P electrons for the Fe_2O_3-N/C (Fe-Phen/C-800) catalyst.

S9. EPR and Mössbauer spectral mesurments of Fe_2O_3-N/C (Fe-Phen/C-800) catalyst

The material Fe_2O_3-N/C (Fe-Phen/C-800) shows broad anisotropic signals at low temperature which are characteristic for the presence of ferromagnetic domains/particles of different size and/or shape (Fig. S4). The magnetic moments of such particles tend to align to the static magnetic field of the spectrometer at low temperature. However, with rising temperature thermal fluctuations of the magnetic moments became dominant which lift this alignment and gave rise to isotropic signals above the so-called blocking temperature T_b. This effect is called super-paramagnetic resonance.[5] The smaller the particle dimension, the lower is T_B and is may be above 380 K since the anisotropy of the signal is still persistent (Fig. S4).

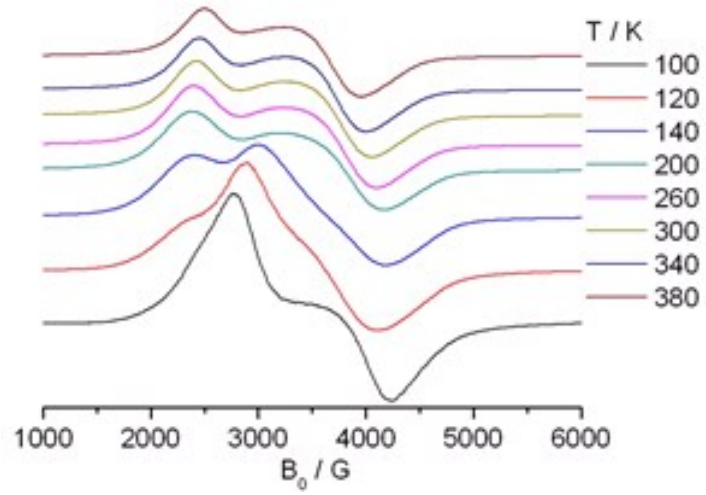

Fig. S4. EPR spectra of Fe_2O_3-N/C (Fe-Phen/C-800) catalyst measured as a function of temperature

By EPR spectroscopy alone it is not possible to identify the phase of the superparamagnetic particles. Given the thermal pre-treatment in argon atmosphere rather the formation of zero-valent iron than of ferric oxide particles was expected. Since EPR can hardly distinguish between ferromagnetic and/or superparamagnetic particles of those phases, Mössbauer spectra have been recorded in addition (Fig. S5). In the Mössbauer spectra, C1 turns into a magnetically split sextet with hyperfine field of B_{hf} = 50.5 T and 50.3 T at 300 K, which comprises about 50 % and 71 % at 77 K, respectively, of all Fe species. The hyperfine field is comparable to that of γ-Fe_2O_3.[6] Besides, sample contains a minor amount of high-spin Fe(II) reflected by component C3. In all samples, the presence of metallic iron phases or iron carbide can be excluded. Metallic iron phases would exhibit a magnetic hyperfine field of 33 T at room temperature and carbidic iron phases would have even less hyperfine fields. Moreover, the observed isomer shifts do not agree with the expected values for such phases. Based on EPR and Mössbauer results it can be concluded that thermal pre-treatment and subsequent exposure of the catalyst to ambient atmosphere at room temperature leads to the formation of super-paramagnetic Fe_2O_3 particles, the relative percentage (with respect to the total Fe content) and the size of which increases with rising pre-treatment temperature. This agrees properly with the TEM results. Given that thermal pre-treatment has been performed in the absence of oxygen, it is possible that metallic Fe was formed initially but oxidized quickly upon contact with ambient atmosphere. More likely, oxygen from the acetate ligands is directly incorporated.

Table S1. Isomer shifts δ, quadrupole splitting ΔE_Q, hyperfine field B_{hf} and relative intensity I_{rel} as obtained by the analysis of the Mössbauer spectra plotted in Fig. S5

Catalyst	T / K	Component	δ / mm s^{-1}	ΔE_Q / mm s^{-1}	I_{rel} / %	B_{hf} / T
Fe_2O_3-N/C	300	C1	0.35	0	71	50.3
		C2	0.38	1.00	29	
	77	C1	0.4	0	56	52.4
		C2	0.48	1.00	44	

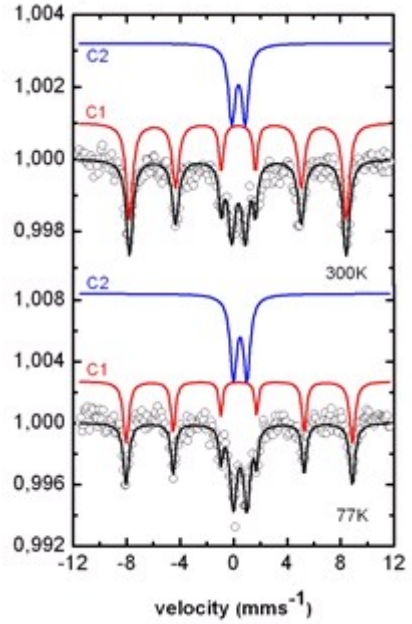

Fig. S5. Mössbauer spectra of Fe_2O_3-N/C catalyst measured at 300 and 77 K. The solid lines have been calculated assuming doublets and sextets with lorentzian line shape

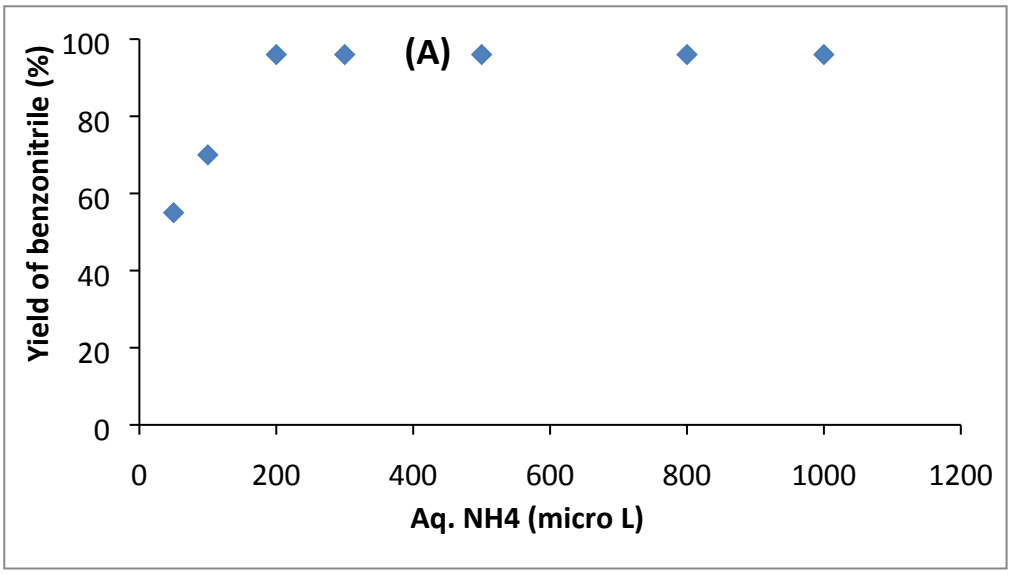
(A)
Yield of benzonitrile (%)
100
80
60
40
20
0
0
200
400
600
800
1000
1200
Aq. NH4 (micro L)

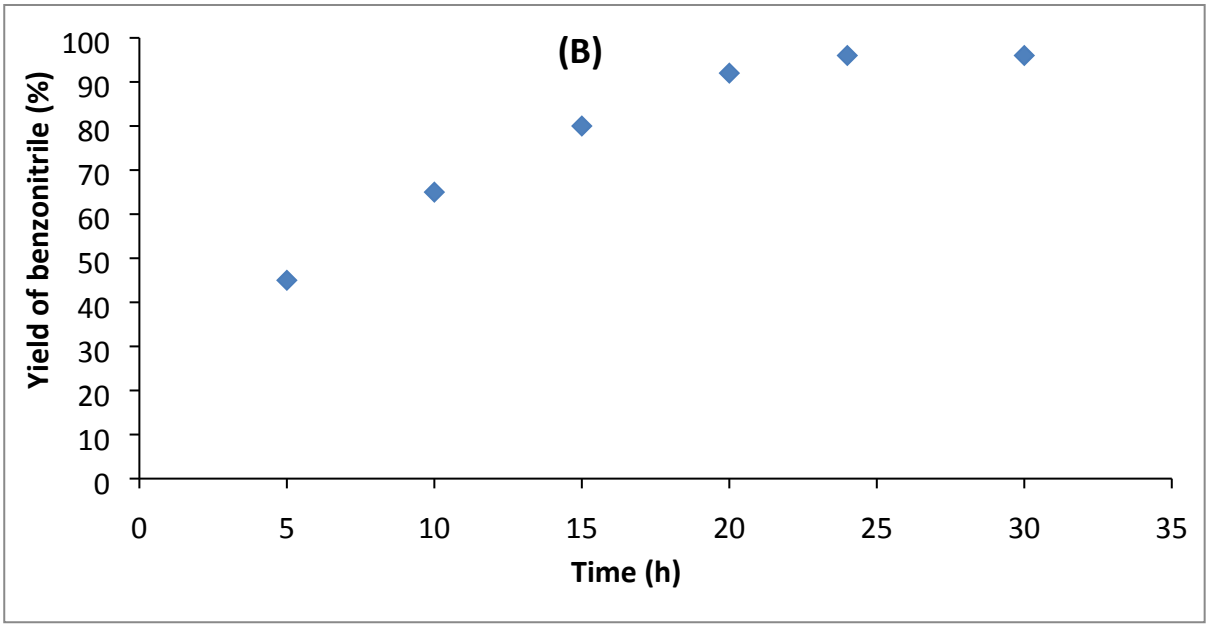
(B)
Yield of benzonitrile (%)
100
90
80
70
60
50
40
30
20
10
0
0
5
10
15
20
25
30
35
Time (h)

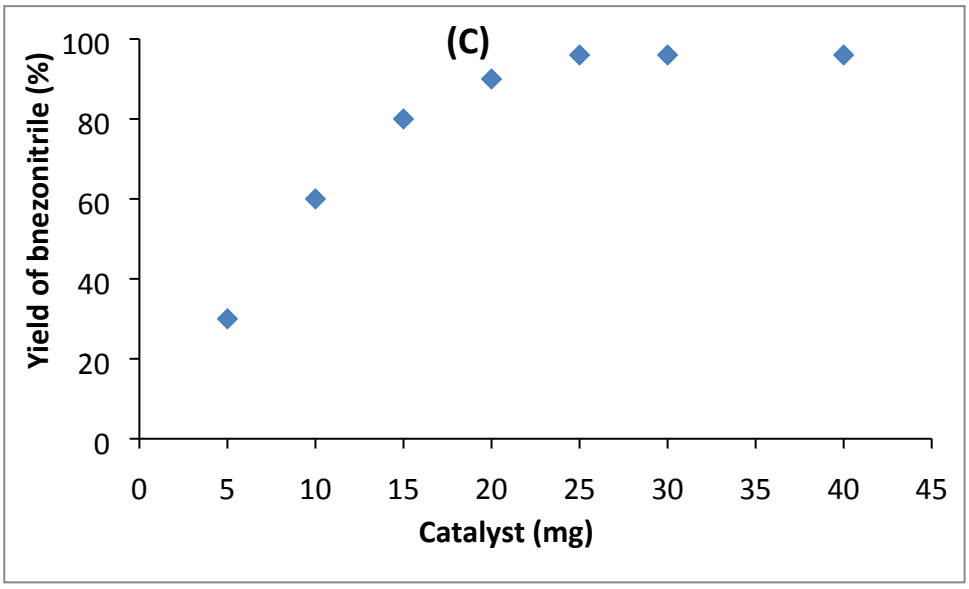
(C)
Yield of bnezonitrile (%)
100
80
60
40
20
0
0
5
10
15
20
25
30
35
40
45
Catalyst (mg)

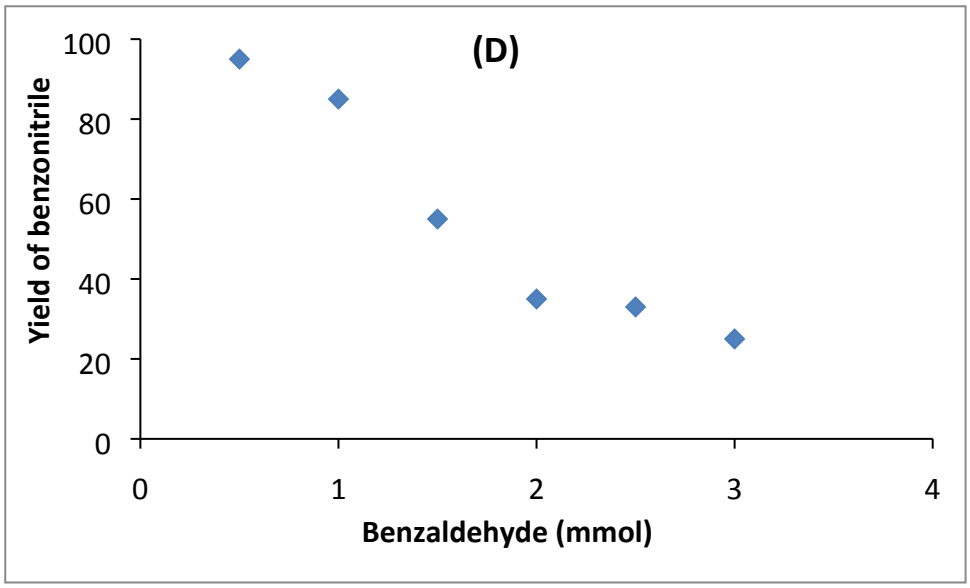

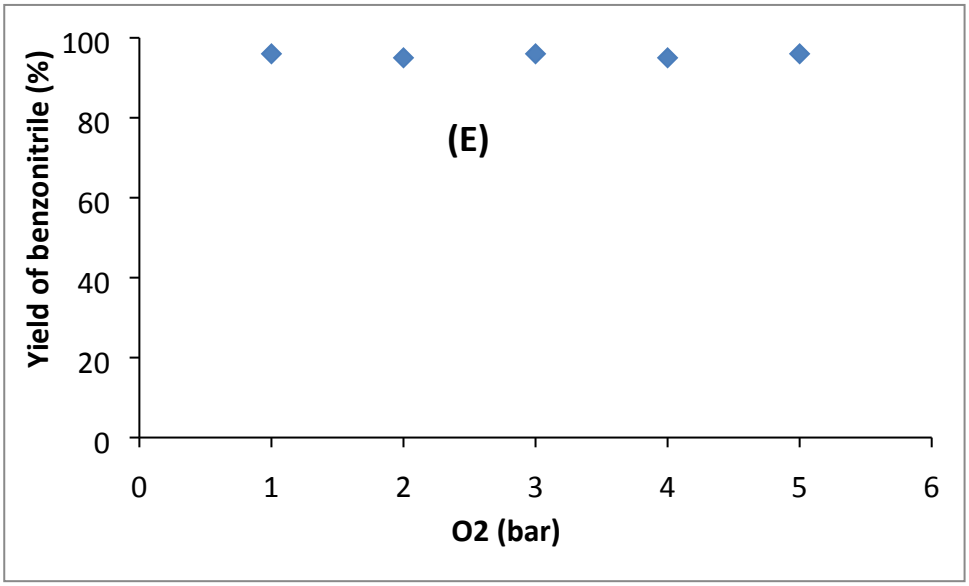

Fig. S6. Kinetics plots of yield of benzonitriles Vs. Aq. NH_3 (A), time (B), catalyst (C), concentration of benzaldehyde (D) and pressure oxygen (E).

Reaction conditions: (A) = 0.5 mmol benzaldehyde, 50-1000 µL aq. NH_3 (28-30% NH_3 basis), 30 mg catalyst (3 mol% Fe), 1 bar O_2 (balloon), 2 mL t-amyl alcohol, 40 °C, 24 h. (B)= 0.5 mmol benzaldehyde, 200 µL aq. NH_3 (28-30% NH_3 basis), 30 mg catalyst (3 mol% Fe), 1 bar O_2 (balloon), 2 mL t-amyl alcohol, 40 °C, 5-30 h. (C)= 0.5 mmol benzaldehyde, 200 µL aq. NH_3 (28-30% NH_3 basis), 5-40 mg catalyst (3 mol% Fe), 1 bar O_2 (balloon), 2 mL t-amyl alcohol, 40 °C, 24 h. (D)= 0.5-3.0 mmol benzaldehyde, 200 µL aq. NH_3 (28-30% NH_3 basis), 30 mg catalyst (3 mol% Fe), 1 bar O_2 (balloon), 2 mL t-amyl alcohol, 40 °C, 24 h. (E)= 0.5 mmol benzaldehyde, 200 µL aq. NH_3 (28-30% NH_3 basis), 30 mg catalyst (3 mol% Fe), 1-5 bar O_2 (balloon), 2 mL t-amyl alcohol, 40 °C, 24 h.

S10. NMR data

KM11-11

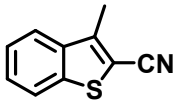

^{1}H NMR (300 MHz, Chloroform-*d*) δ 7.78 – 7.62 (m, 2H), 7.53 – 7.26 (m, 2H), 2.52 (s, 3H). **^{13}C NMR (75 MHz, Chloroform-*d*)** δ 145.22 , 140.78 , 137.55 , 127.92 , 125.35 , 123.52 , 122.66 , 114.57 , 105.59 , 13.75 . Yellow solid.

KM11-17

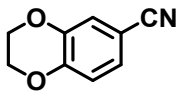

^{1}H NMR (300 MHz, Chloroform-*d*) δ 7.17 – 6.96 (m, 2H), 6.93 – 6.70 (m, 1H), 4.33 – 4.11 (m, 4H). **^{13}C NMR (75 MHz, Chloroform-*d*)** δ 147.75 , 143.80 , 125.87 , 121.21 , 118.91 , 118.25 , 104.38 , 64.59 , 64.12 . Off white solid

KM11-21

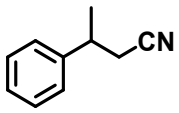

^{1}H NMR (300 MHz, Chloroform-*d*) δ 7.38 – 6.96 (m, 5H), 3.19 – 2.89 (m, 1H), 2.61 – 2.31 (m, 2H), 1.37 (d, *J* = 7.0 Hz, 3H). **^{13}C NMR (75 MHz, Chloroform-*d*)** δ 143.16 , 128.88 , 127.35 , 126.57 , 118.63 , 36.55 , 26.36 , 20.70 . Yellow gum.

KM11-27

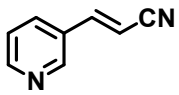

^{1}H NMR (300 MHz, Chloroform-*d*) δ 8.62 (d, *J* = 3.0 Hz, 1H), 8.59 (dd, *J* = 4.9, 1.6 Hz, 1H), 7.74-7.72 (m, 1H), 7.39 – 7.26 (m, 2H), 5.92 (d, *J* = 16.7 Hz, 1H). **^{13}C NMR (75 MHz, Chloroform-*d*)** δ 151.89 , 148.99 , 147.02 , 133.53 , 129.30 , 123.89 , 117.35 , 98.82 . Pale yellow solid.

KM11-28

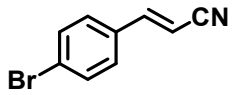

^{1}H NMR (300 MHz, Chloroform-*d*) δ (d, *J* = 9 Hz, 2H), 7.29 – 7.19 (m, 3H), 5.80 (d, *J* = 16.6 Hz, 1H). **^{13}C NMR (75 MHz, Chloroform-*d*)** δ 149.20 , 132.49 , 132.37 , 128.73 , 125.62 , 117.84 , 97.10 . Yellow solid.

KM11-32

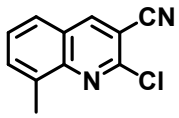

^{1}H NMR (300 MHz, Chloroform-*d*) δ 8.37 (s, 1H), 7.62 (m, 2H), 7.47 (dd, *J* = 8.2, 7.0 Hz, 1H), 2.64 (s, 3H). **^{13}C NMR (75 MHz, Chloroform-*d*)** δ 147.29 , 147.01 , 144.95 , 137.31 , 134.02 , 128.46 , 125.92 , 125.14 , 115.31 , 107.40 , 17.63 . Yellow solid.

KM11-54

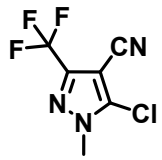

^{1}H NMR (300 MHz, Chloroform-*d*) δ 3.90 (s, 3H). **^{13}C NMR (75 MHz, Chloroform-*d*)** δ 143.20 (q, *J* = 212.0 Hz), 135.50 , 119.07 (q, *J* = 270.7 Hz), 108.90 , 91.42 , 37.87 . Colorless oil.

KM11-57

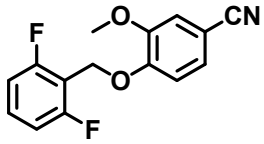

^{1}H NMR (300 MHz, Chloroform-*d*) δ 7.28 – 7.13 (m, 3H), 7.04 – 6.89 (m, 3H), 5.18 (s, 2H), 3.76 (s, 3H). **^{13}C NMR (75 MHz, Chloroform-*d*)** δ 162.07 (d, *J* = 252.0 Hz), 152.03 , 150.00 , 131.16 (d, *J* = 9.9 Hz), 126.24 , 125.67 (d, *J* = 3.5 Hz), 119.17 , 114.82 , 114.43 (d, *J* = 22.5 Hz), 113.91 , 104.76 , 62.33 (d, *J* = 4.1 Hz), 56.27 . White solid.

KM11-230

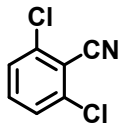

^{1}H NMR (300 MHz, Chloroform-*d*) δ 7.67 – 7.03 (m, 3H). **^{13}C NMR (75 MHz, Chloroform-*d*)** δ 138.43 , 134.00 , 128.21 , 114.31 , 113.35 . White solid.

KM11-58

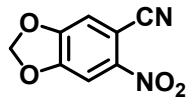

^{1}H NMR (300 MHz, DMSO-d_6) δ 7.94 (s, 1H), 7.73 (s, 1H), 6.39 (s, 2H). **^{13}C NMR (75 MHz, DMSO-d_6)** δ 152.93 , 152.19 , 145.13 , 115.89 , 113.50 , 106.59 , 105.62 , 102.06 . Yellow solid.

KM11-3

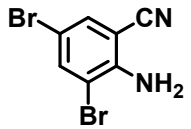

^{1}H NMR (300 MHz, Chloroform-*d*) δ 7.65 (d, *J* = 2.2 Hz, 1H), 7.40 (d, *J* = 2.2 Hz, 1H), 4.84 (br s, 2H). **^{13}C NMR (75 MHz, Chloroform-*d*)** δ 146.21 , 139.38 , 133.60 , 115.61 , 109.74 , 108.20 , 97.90 . White solid.

KM11-4

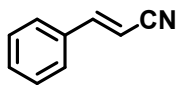

^{1}H NMR (300 MHz, Chloroform-*d*) δ 7.55 – 7.00 (m, 6H), 5.78 (d, *J* = 16.7 Hz, 1H). **^{13}C NMR (75 MHz, Chloroform-*d*)** δ 150.59 , 133.52 , 131.25 , 129.14 , 127.40 , 118.22 , 96.35 . Colorless oil.

KM11-12

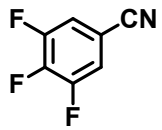

^{1}H NMR (300 MHz, Chloroform-*d*) δ 7.45 – 7.01 (m, 2H). **^{13}C NMR (75 MHz, DMSO-d_6)** δ 151.46 (ddd, *J* = 236.6, 9.8, 3.5 Hz), 143.44 (dt, *J* = 243.6, 13.3 Hz), 117.34 (dt, *J* = 23.1, 8.4 Hz), 115.93 (t, *J* = 2.8 Hz), 108.0 (td, *J* = 14.0, 4.9 Hz). Colorless gum.

KM11-34

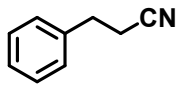

^{1}H NMR (300 MHz, Chloroform-*d*) δ 7.46 – 6.89 (m, 5H), 2.85 (t, *J* = 7.4 Hz, 2H), 2.50 (t, *J* = 6.0 Hz, 2H). **^{13}C NMR (75 MHz, Chloroform-*d*)** δ 138.12 , 128.89 , 128.31 , 127.25 , 119.23 , 31.57 , 19.36 . Colorless oil.

KM11-53

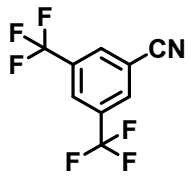

^{1}H NMR (300 MHz, Chloroform-*d*) δ 8.95 – 8.10 (m, 3H). **^{13}C NMR (75 MHz, Chloroform-*d*)** δ 133.23 (q, *J* = 34.8 Hz), 132.22 (q, *J* = 3.8 Hz), 125.75 (q, *J* = 253.4 Hz) 126.48 (hept, *J* = 3.3 Hz), 115.89 , 114.87 . Colorless oil.

KM11-79

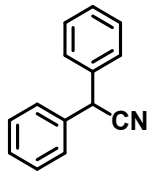

^{1}H NMR (300 MHz, Chloroform-*d*) δ 7.44 – 7.15 (m, 10H), 5.05 (s, 1H). **^{13}C NMR (75 MHz, Chloroform-*d*)** δ 135.92 , 129.22 , 128.28 , 127.75 , 119.72 , 42.62 . Pale Yellow solid.

KM11-95

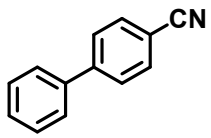

^{1}H NMR (300 MHz, Chloroform-*d*) δ 7.64 – 7.55 (m, 4H), 7.52 – 7.46 (m, 2H), 7.42 – 7.29 (m, 3H). **^{13}C NMR (75 MHz, Chloroform-*d*)** δ 145.66 , 139.16 , 132.61 , 129.14 , 128.69 , 127.74 , 127.24 , 118.98 , 110.91 . White solid.

KM11-70

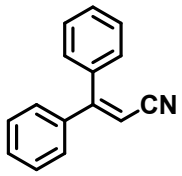

^{1}H NMR (300 MHz, Chloroform-*d*) δ 7.65 – 6.95 (m, 10H), 5.62 (s, 1H). **^{13}C NMR (75 MHz, Chloroform-*d*)** δ 163.15 , 138.94 , 137.10 , 130.50 , 130.09 , 129.61 , 128.72 , 128.61 , 128.53 , 117.98 , 94.95 .

KM11-74 (cis trans isomer mixture)

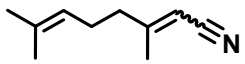

^{1}H NMR (300 MHz, Chloroform-*d*) δ 5.19 – 4.75 (m, 2H), 2.41 – 2.26 (m, 1H), 2.20 – 2.04 (m, 3H), 1.91 (m, 3H), 1.62 (dt, *J* = 2.5, 1.3 Hz, 3H), 1.58 – 1.50 (m, 3H). **^{13}C NMR (75 MHz, Chloroform-*d*)** δ 165.13 , 165.02 , 133.32 , 133.20 , 122.21 , 122.16 , 117.28 , 116.98 , 95.80 , 95.22 , 38.57 , 36.28 , 26.13 , 25.65 , 25.62 , 25.60 , 22.90 , 21.03 , 17.72 , 17.66 .

KM11-76

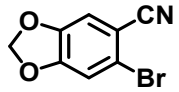

^{1}H NMR (300 MHz, Chloroform-*d*) δ 7.00 (s, 1H), 6.94 (s, 1H), 6.04 (s, 2H). **^{13}C NMR (75 MHz, Chloroform-*d*)** δ 152.28 , 147.49 , 118.90 , 117.36 , 113.36 , 112.50 , 107.80 , 103.17 . White solid

KM11-77

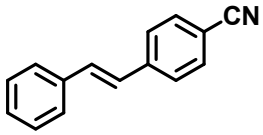

^{1}H NMR (300 MHz, Chloroform-*d*) δ 7.53 – 7.37 (m, 6H), 7.33 – 7.16 (m, 3H), 7.09 (d, *J* = 16.4 Hz, 1H), 6.95 (d, *J* = 16.4 Hz, 1H). **^{13}C NMR (75 MHz, Chloroform-*d*)** δ 141.83 , 136.30 , 132.52, 132.40 , 128.89 , 128.68 , 126.96 , 126.89 , 126.72 , 119.10 , 110.54 . White solid.

KM11-142

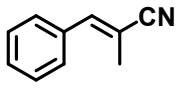

^{1}H NMR (300 MHz, Chloroform-*d*) δ 7.36 – 7.19 (m, 5H), 7.11 – 7.10 (m, 1H), 2.04 (s, 3H). **^{13}C NMR (75 MHz, Chloroform-*d*)** δ 144.43 , 133.94 , 129.35 , 129.32 , 128.71 , 121.13 , 109.49 , 16.82 . Pale Yellow gum.

KM11-144

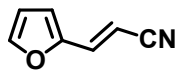

^{1}H NMR (300 MHz, Chloroform-*d*) δ 7.48-7.72 (m, 1H), 7.03 (d, *J* = 20.00 Hz, 1H), 6.41-6.55 (m, 2H), 5.68 (d, *J* = 20.00 Hz, 1H). **^{13}C NMR (75 MHz, Chloroform-*d*)** δ 149.79 , 145.47 , 136.15 , 118.28 , 115.47 , 112.64 , 93.34 . Brown gum.

KM11-146

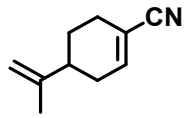

^{1}H NMR (300 MHz, Chloroform-*d*) δ 6.58 (m,1H), 4.74 – 4.70 (m, 1H), 4.64 (m, 1H), 2.32 – 2.19 (m, 3H), 2.14 – 2.03 (m, 2H), 1.86 – 1.77 (m, 1H), 1.69 – 1.65 (m, 3H), 1.52 – 1.39 (m, 1H). **^{13}C NMR (75 MHz, Chloroform-*d*)** δ 147.72 , 144.62 , 119.53 , 112.06 , 109.84 , 39.20 , 30.96 , 26.93 , 26.28 , 20.63 . Yellow oil.

KM11-148

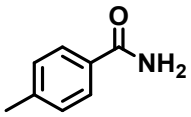

^{1}H NMR (300 MHz, DMSO-d_6) δ 7.91 (br s, 1H), 7.8 (d, *J* = 6.00 Hz, 2H), 7.28 (br s, 1H), 7.2 (d, *J* = 9.00 Hz, 2H), 2.34 (s, 3H). **^{13}C NMR (75 MHz, DMSO-d_6)** δ 168.32 , 141.50 , 131.96 , 129.18 , 127.98 , 21.39 . White solid.

KM11-162

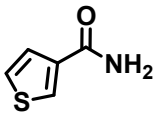

^{1}H NMR (300 MHz, DMSO-d_6) δ 8.14 (dd, *J* = 3.0, 1.3 Hz, 1H), 7.78 (br s, 1H), 7.56 (dd, *J* = 5.0, 2.9 Hz, 1H), 7.49 (dd, *J* = 5.0, 1.3 Hz, 1H), 7.23 (br s, 1H). **^{13}C NMR (75 MHz, DMSO-d_6)** δ 164.16 , 138.47 , 129.45 , 127.62 , 126.99 . Offwhite solid.

KM11-190

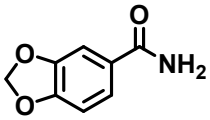

^{1}H NMR (300 MHz, DMSO-d_6) δ 7.81 (br s, 1H), 7.48 (dd, *J* = 8.1, 1.8 Hz, 1H), 7.41 (dd, *J* = 1.8, 0.4 Hz, 1H), 7.23 (br s, 1H), 6.97 (d, *J* = 9.0 Hz, 1H), 6.09 (s, 2H). **^{13}C NMR (75 MHz, DMSO-d_6)** δ 167.45 , 150.14 , 147.70 , 128.77 , 122.96 , 108.19 , 108.02 , 102.05 . Yellow solid.

KM11-196

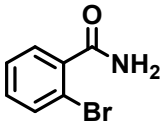

^{1}H NMR (300 MHz, DMSO-d_6) δ 7.87 (br s, 1H), 7.69 – 7.62 (m, 1H), 7.58 (br s, 1H), 7.46 – 7.39 (m, 2H), 7.35 – 7.31 (m, 1H). **^{13}C NMR (75 MHz, DMSO-d_6)** δ 169.54 , 139.81 , 133.18 , 131.11 , 129.03 , 127.95 , 119.09 . White solid

KM11-197

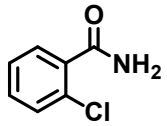

^{1}H NMR (300 MHz, DMSO-d_6) δ 7.89 (br s, 1H), 7.60 (br s, 1H), 7.54 – 7.34 (m, 4H). **^{13}C NMR (75 MHz, DMSO-d_6)** δ 168.67 , 137.60 , 131.02 , 130.14 , 130.07 , 129.14 , 127.47 . White solid

KM11-198

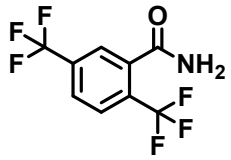

^{1}H NMR (300 MHz, DMSO-d_6) δ 8.17 (br s, 1H), 8.02 (dd, *J* = 1.8, 0.7 Hz, 2H), 7.91 – 7.80 (m, 1H), 7.83 (br s, 1H). **^{13}C NMR (75 MHz, DMSO-d_6)** δ 167.98 , 138.32 (q, *J* = 2.1 Hz), 132.90 (q, *J* = 32.6 Hz), 129.90 (q, *J* = 33.4 Hz), 128.19 (q, *J* = 4.9 Hz), 126.94 (q, *J* = 3.7 Hz), 125.67 (q, *J* = 3.8 Hz), 123.39 (q, *J* = 253.4 Hz), 123.21 (q, *J* = 254.8 Hz)).Yellow soild

KM11-199

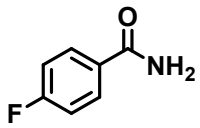

^{1}H NMR (300 MHz, DMSO-d_6) δ 8.04 – 7.92 (m, 3H), 7.41 (br s, 1H), 7.32 – 7.23 (m, 2H). **^{13}C NMR (75 MHz, DMSO-d_6)** δ 167.35 , 164.39 (d, *J* = 248.4 Hz), 131.20 (d, *J* = 2.9 Hz), 130.57 (d, *J* = 9.0 Hz), 115.52 (d, *J* = 21.7 Hz). White solid.

KM11-202

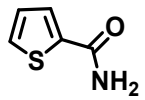

^{1}H NMR (300 MHz, DMSO-d_6) δ 7.99 (br s, 1H), 7.80 – 7.68 (m, 2H), 7.40 (br s, 1H), 7.13 (m, 1H). **^{13}C NMR (75 MHz, DMSO-d_6)** δ 163.44 , 140.73 , 131.41 , 129.18 , 128.34 . White solid.

KM11-205

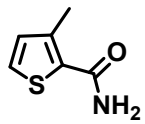

^{1}H NMR (300 MHz, DMSO-d_6) δ 7.54 (d, *J* = 8.0, Hz, 1H), 7.34 (br s, 2H), 6.94 (d, *J* = 8.0, Hz, 1H), 2.43 (s, 3H). **^{13}C NMR (75 MHz, DMSO-d_6)** δ 164.63 , 140.41 , 132.34 , 132.04 , 127.72 , 15.79 . White solid.

KM11-214

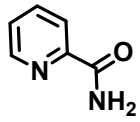

^{1}H NMR (300 MHz, DMSO-d_6) δ 8.61 (dt, *J* = 3.2, 1.9 Hz, 1H), 8.17 (br s, 1H), 8.11 – 8.03 (m, 1H), 8.01 – 7.90 (m, 1H), 7.71 (br s, 1H), 7.56 – 7.53 (m, 1H). **^{13}C NMR (75 MHz, DMSO-d_6)** δ 166.58 , 150.73 , 148.86 , 138.04 , 126.86 , 122.37 . White solid.

KM11-211

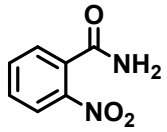

^{1}H NMR (300 MHz, DMSO-d_6) δ 8.17 (br s, 1H), 8.01 (ddd, *J* = 8.0, 1.3, 0.5 Hz, 1H), 7.82 – 7.73 (m, 1H), 7.73 – 7.60 (m, 3H). **^{13}C NMR (75 MHz, DMSO-d_6)** δ 167.69 , 147.69 , 133.78 , 133.06 , 131.06 , 129.30 , 124.39 . White solid.

KM11-211

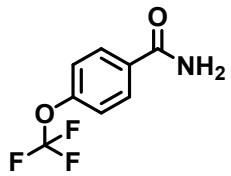

^{1}H NMR (300 MHz, DMSO-d_6) δ 13.22 (br s, 1H), 8.07 (d, *J* = 9.0, Hz, 2H), 7.48 (d, *J* = 6.0, Hz, 2H), 3.33 (br s, 1H). **^{13}C NMR (75 MHz, DMSO-d_6)** δ 166.62 , 151.90 , 132.15 , 130.33 , 125.29 (q, *J* = 238.7 Hz), 121.15 . White solid.

S11. References

1. F. Jaouen, *et al.*, *ACS Appl. Mater. Interfaces*, **2009,** *1*, 1623-1639.
2. F. Buchner, K. Flechtner, Y. Bai, E. Zillner, I. Kellner, H. Steinrück, H. Marbach, J. M. Gottfried, *J. Phys. Chem. C*, **2008**, *112*, 15458-15465.
3. (a) M. Descostes, F. Mercier, N. Thromat, C. Beaucaire, M. Gautier-Soyer, *Appl.Surf. Sci.* **2000**, *165*, 288-302; (b) J.F. Moulder, W.F. Stickle, P.E. Sobol, K.D. Bomben, Handbook of X-ray Photoelectron Spectroscopy, Perkin-Elmer Corp., Eden Praire, MN, 1992.
4. (a) M. Stöcker, *Microporous Mater*. **1996**, *6*, 235–257; (b) P. Grosvenor, B.A. Kobe, M.C. Biesinger, N.S. McIntyre, *Surf. Interface Anal.* **2004**, *36*, 1564–1574.
5. R. Berger, J-C. Bissey, J. Kliava, H. Daubric, C. Estournès, *J. Magn. Mater.* **2001**, *234,* 535.
6. H. Huang, R. Christmann, R. Ulber, V. Schünemann, *Hyperfine Interactions*, **2012** *205*, 121–124

S12. NMR spectra

170524.316.1.fid
Kathir KM11-11
Au1H CDCl3 {C:\Bruker\TopSpin3.5pl6} 1705 16

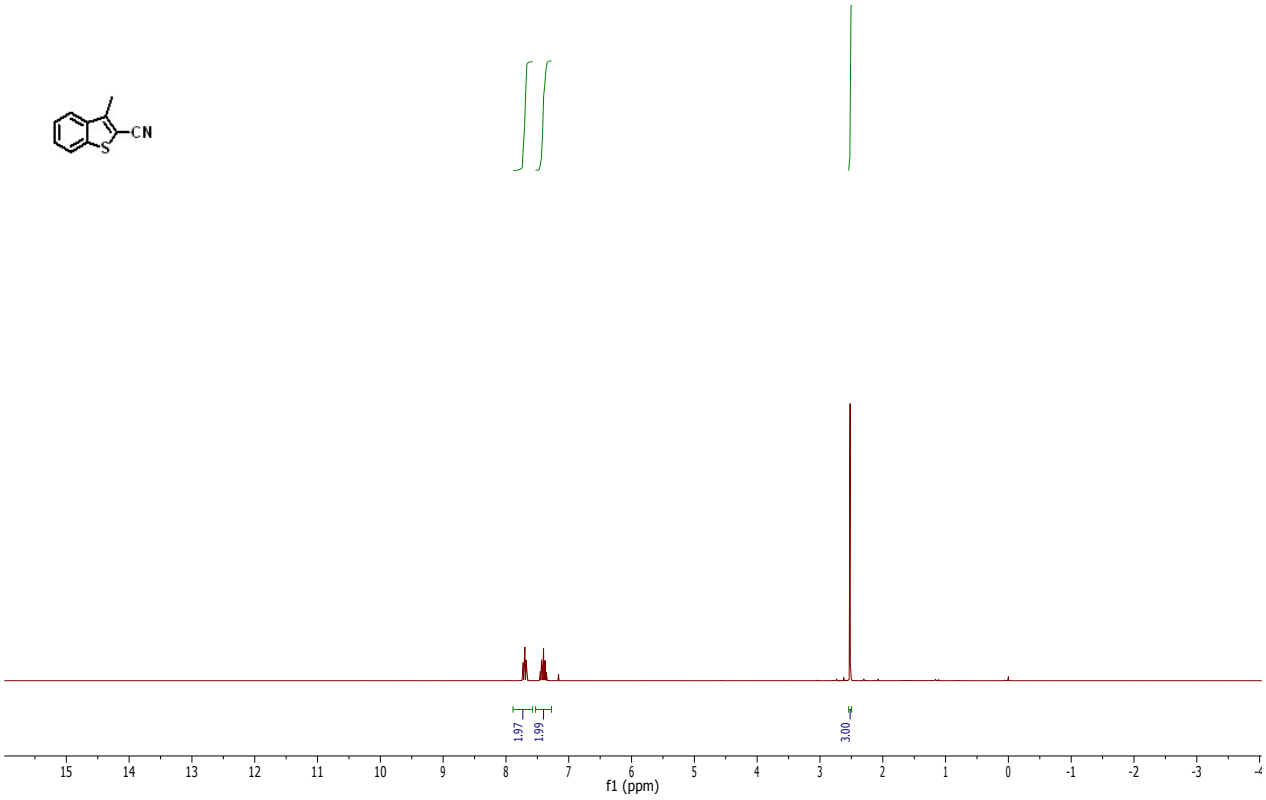

170524.316.2.fid
Kathir KM11-11
Au13C CDCl3 {C:\Bruker\TopSpin3.5pl6} 1705 16

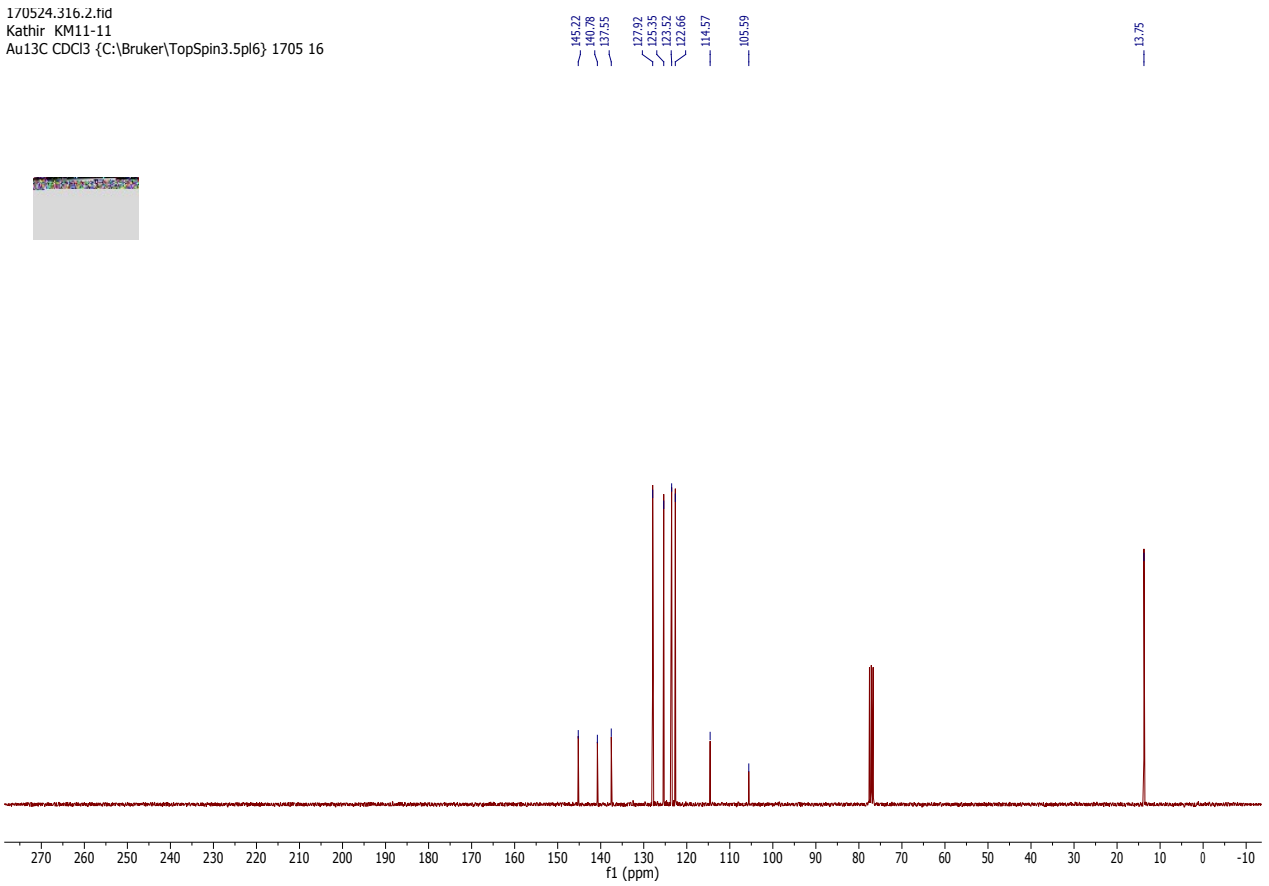

170524.317.1.fid
Kathir KM11-17
Au1H CDCl3 {C:\Bruker\TopSpin3.5pl6} 1705 17

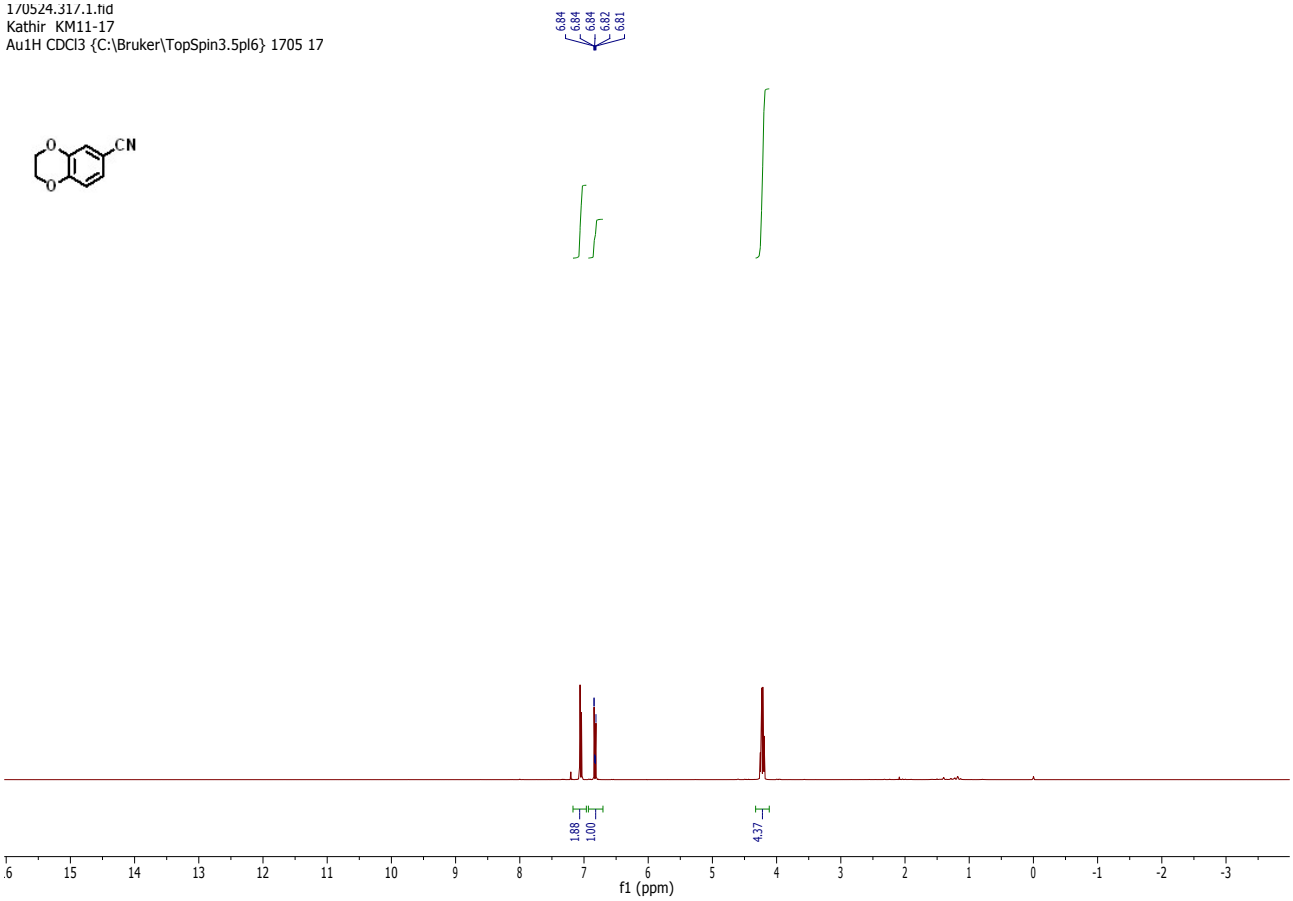

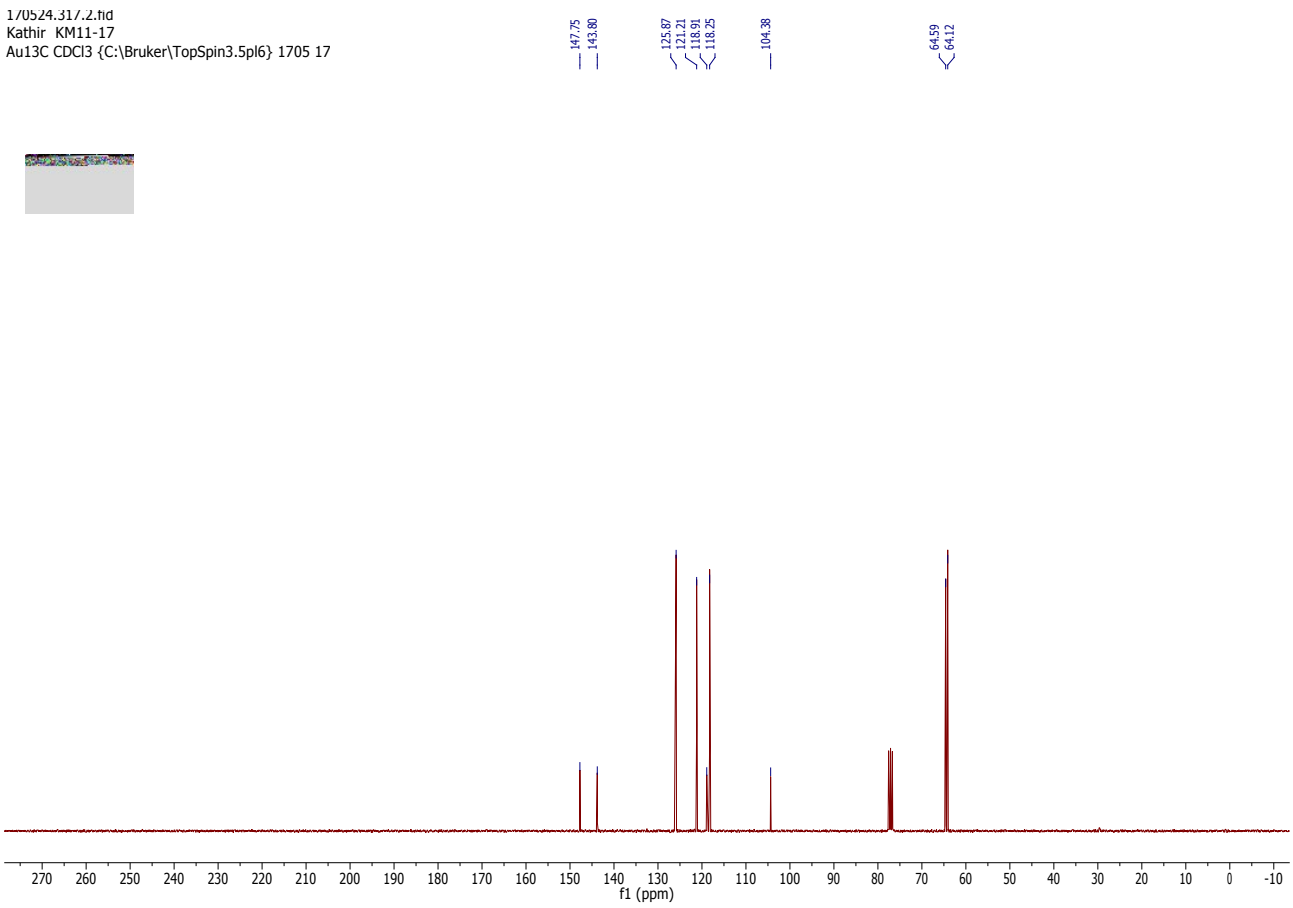
1705241317.2.fid
Kathir KM11-17
Au13C CDCl3 {C:\Bruker\TopSpin3.5pl6} 1705 17
147.75
143.80
125.87
121.21
118.91
118.25
104.38
64.59
64.12
270 260 250 240 230 220 210 200 190 180 170 160 150 140 130 120 110 100 90 80 70 60 50 40 30 20 10 0 -10
f1 (ppm)

170526.303.1.fid
Kathir KM11-21
Au1H CDCl3 {C:\Bruker\TopSpin3.5pl6} 1705 3

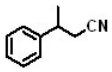

170526.303.2.fid
Kathir KM11-21
Au13C CDCl3 {C:\Bruker\TopSpin3.5pl6} 1705 3

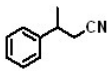

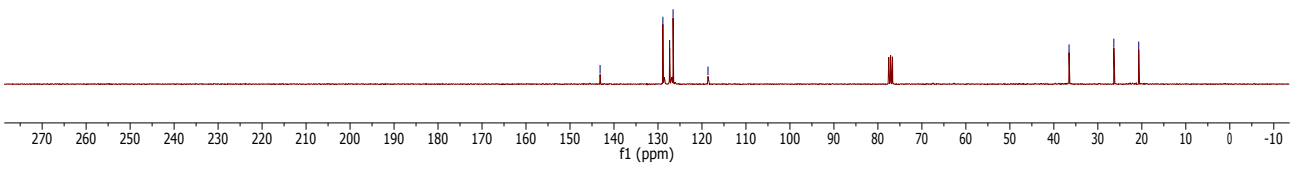

1705265305.1.fid
Kathir KM11-27
Au1H CDCl3 {C:\Bruker\TopSpin3.5pl6} 1705 5

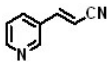

1705265305.2.fid
Kathir KM11-27
Au13C CDCl3 {C:\Bruker\TopSpin3.5pl6} 1705 5

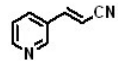

170526.306.1.fid
Kathir KM11-28
Au1H CDCl3 {C:\Bruker\TopSpin3.5pl6} 1705 6

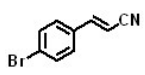

170526.306.2.fid
Kathir KM11-28
Au13C CDCl3 {C:\Bruker\TopSpin3.5pl6} 1705 6

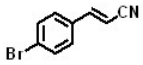

1705263071.fid
Kathir KM11-32
Au1H CDCl3 {C:\Bruker\TopSpin3.5pl6} 1705 7

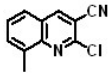

1705263072.fid
Kathir KM11-32
Au13C CDCl3 {C:\Bruker\TopSpin3.5pl6} 1705 7

147.29
147.01
144.95
137.31
134.02
128.46
125.92
125.14
115.31
107.40
17.63

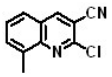

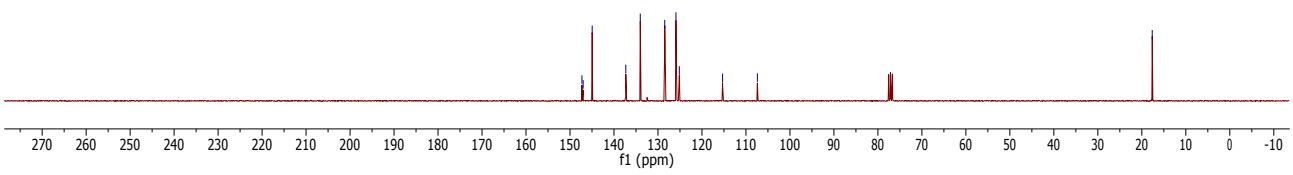

170526.310.1.fid
Kathir KM11-54
Au1H CDCl3 {C:\Bruker\TopSpin3.5pl6} 1705 10

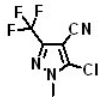

170526.310.2.fid
Kathir KM11-54
Au13C CDCl3 {C:\Bruker\TopSpin3.5pl6} 1705 10

143.99
143.46
142.93
142.40
135.90
124.44
120.86
117.27
113.69
108.90
91.42
37.87

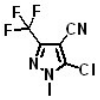

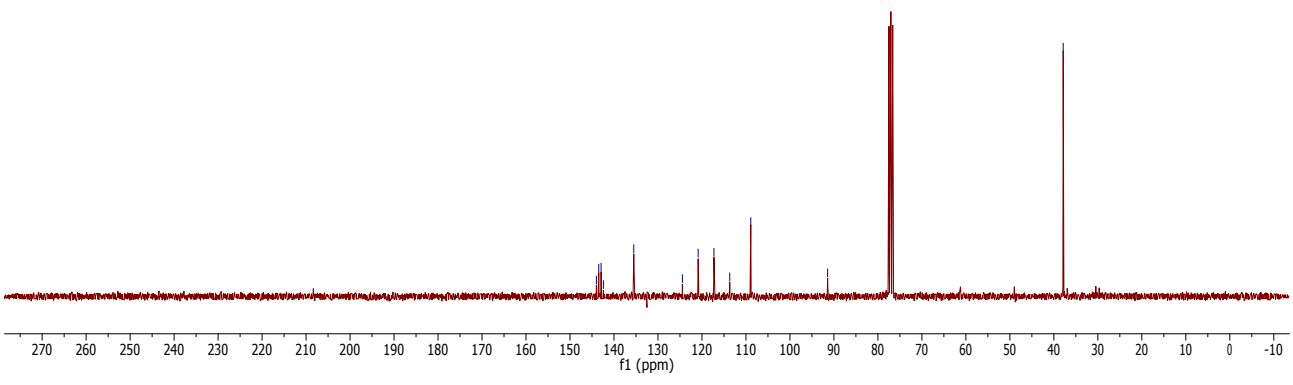

1705261311.1.fid
Kathir KM11-57
Au1H CDCl3 {C:\Bruker\TopSpin3.5pl6} 1705 11

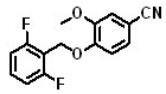

1705261311.2.fid
Kathir KM11-57
Au13C CDCl3 {C:\Bruker\TopSpin3.5pl6} 1705 11

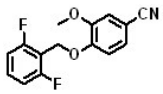

170628.f347.10.fid
Kathir/ KM11-230
PROTON CDCl3 {C:\Bruker\TopSpin3.5pl6} 1706 47

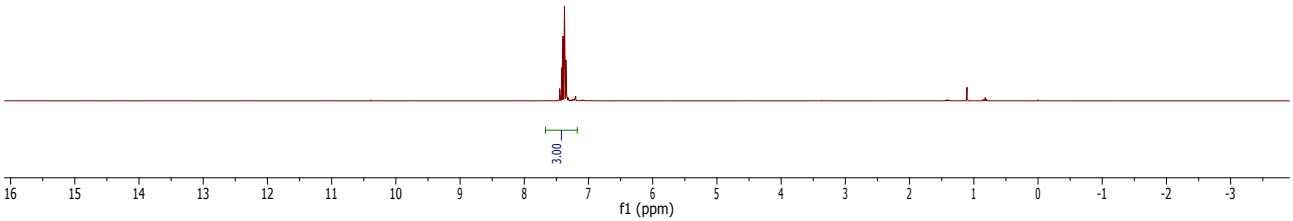

170628.f347.11.fid
Kathir/ KM11-230
C13CPD CDCl3 {C:\Bruker\TopSpin3.5pl6} 1706 47

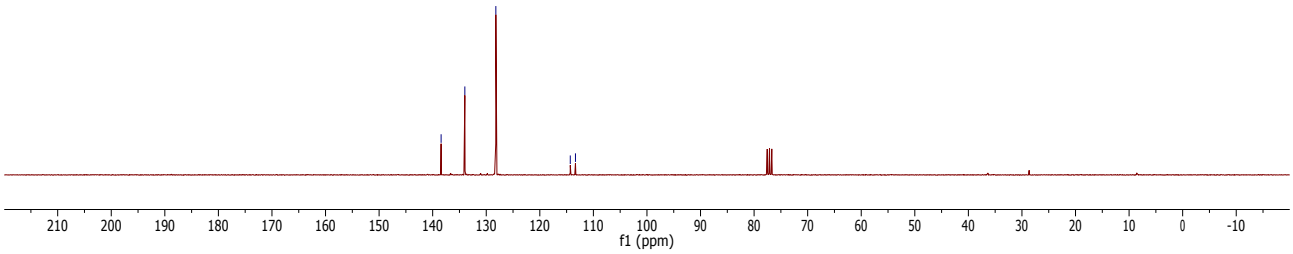

170526.324.1.fid
Kathir KM11-58
Au1H DMSO {C:\Bruker\TopSpin3.5pl6} 1705 24

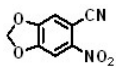

170526.324.2.fid
Kathir KM11-58
Au13C DMSO {C:\Bruker\TopSpin3.5pl6} 1705 24

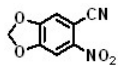

170526.325.1.fid
Kathir KM11-3
Au1H CDCl3 {C:\Bruker\TopSpin3.5pl6} 1705 25

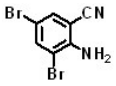

170526.325.2.fid
Kathir KM11-3
Au13C CDCl3 {C:\Bruker\TopSpin3.5pl6} 1705 25

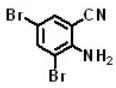

1705 26.326.1.fid
Kathir KM11-4
Au1H CDCl3 {C:\Bruker\TopSpin3.5pl6} 1705 26

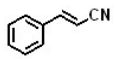

1705 26.326.2.fid
Kathir KM11-4
Au13C CDCl3 {C:\Bruker\TopSpin3.5pl6} 1705 26

170526.327.1.fid
Kathir KM11-12
Au1H CDCl3 {C:\Bruker\TopSpin3.5pl6} 1705 27

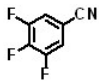

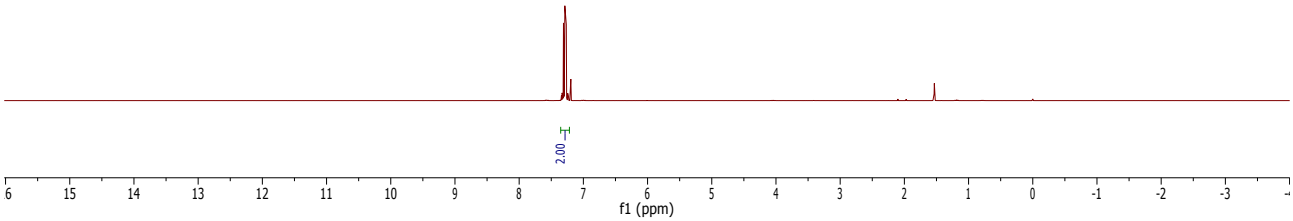

170526.327.2.fid
Kathir KM11-12
Au13C CDCl3 {C:\Bruker\TopSpin3.5pl6} 1705 27

153.25
153.20
153.11
153.06
149.87
149.82
149.73
149.68
145.38
145.19
144.99
141.90
141.71
141.51
117.51
117.39
117.29
117.18
115.90
108.17
108.10
108.04
107.96
107.91
107.83

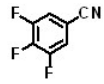

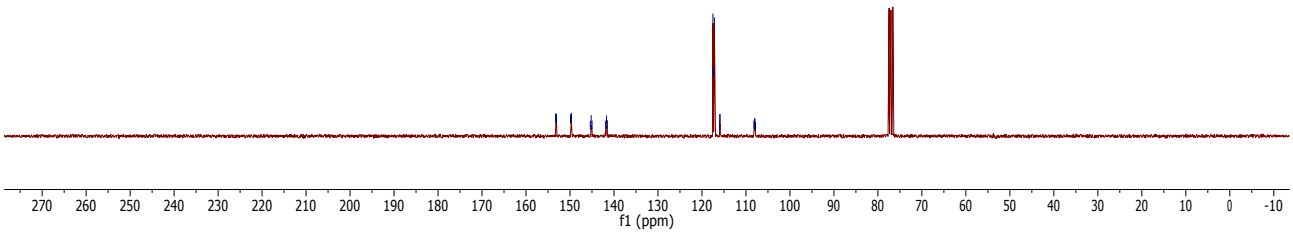

170526.328.1.fid
Kathir KM11-34
Au1H CDCl3 {C:\Bruker\TopSpin3.5pl6} 1705 28

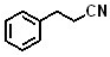

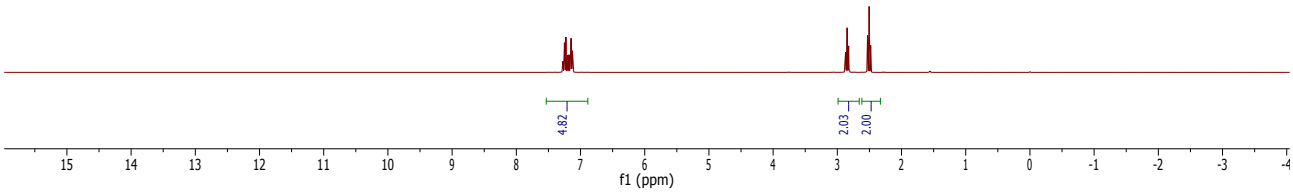

170526.328.2.fid
Kathir KM11-34
Au13C CDCl3 {C:\Bruker\TopSpin3.5pl6} 1705 28

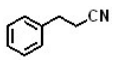

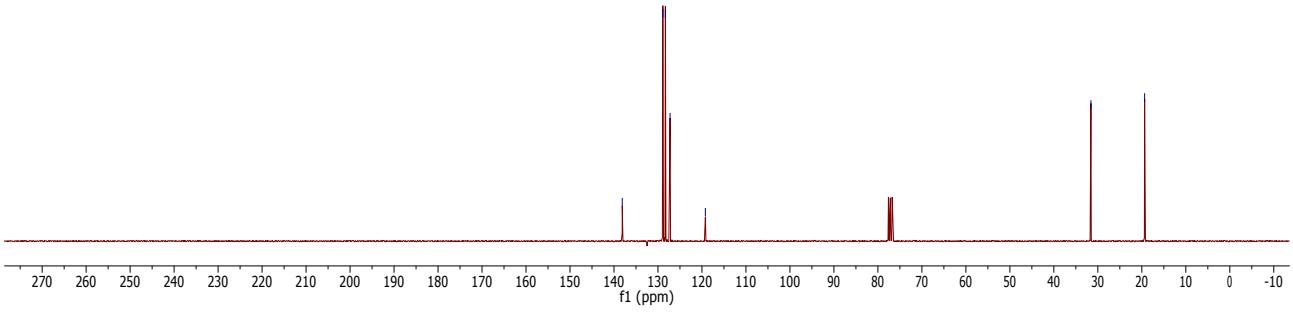

170526.329.1.fid
Kathir KM11-53
Au1H CDCl3 {C:\Bruker\TopSpin3.5pl6} 1705 29

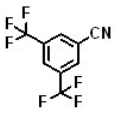

170526.329.2.fid
Kathir KM11-53
Au13C CDCl3 {C:\Bruker\TopSpin3.5pl6} 1705 29

133.93
133.46
133.00
132.54
132.30
132.25
132.20
132.15
127.56
126.62
126.57
126.53
126.48
126.43
126.38
126.34
123.94
120.32
116.70
115.89
114.87

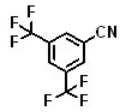

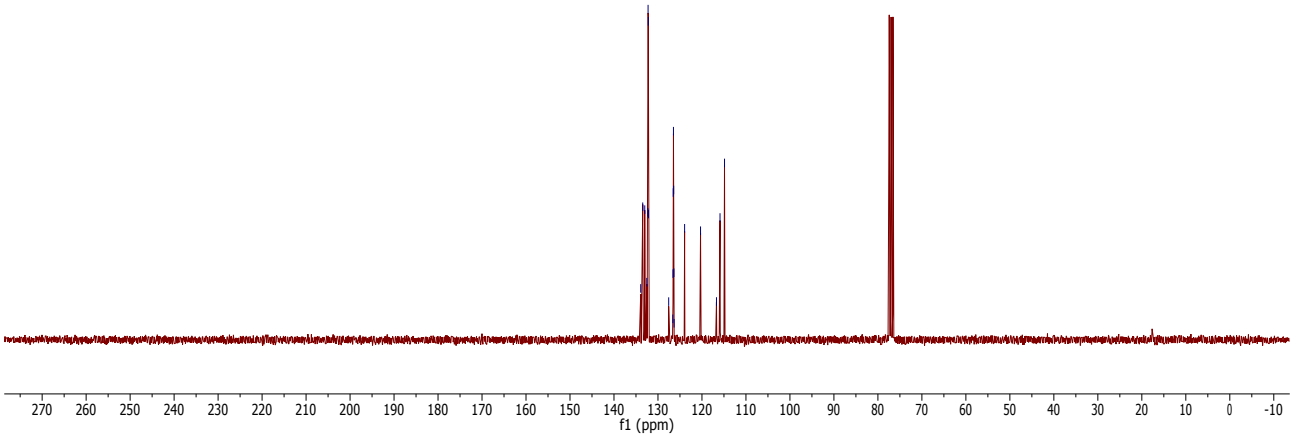

170526.330.1.fid
Kathir KM11-79
Au1H CDCl3 {C:\Bruker\TopSpin3.5pl6} 1705 30

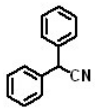

170526.330.2.fid
Kathir KM11-79
Au13C CDCl3 {C:\Bruker\TopSpin3.5pl6} 1705 30

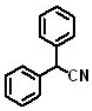

1705263311.fid
Kathir KM11-95
Au1H CDCl3 {C:\Bruker\TopSpin3.5pl6} 1705 31

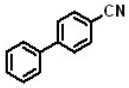

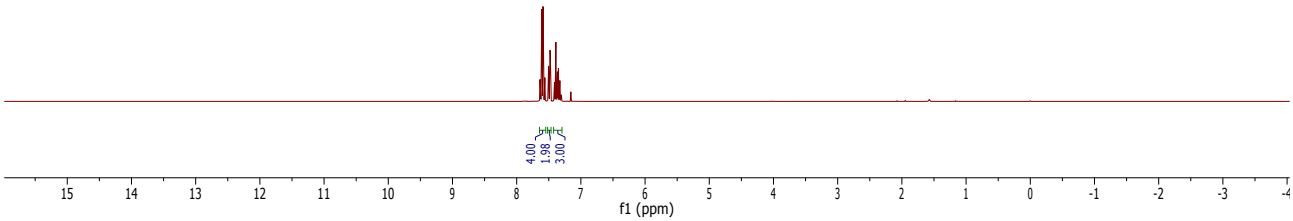

1705263312.fid
Kathir KM11-95
Au13C CDCl3 {C:\Bruker\TopSpin3.5pl6} 1705 31

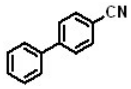

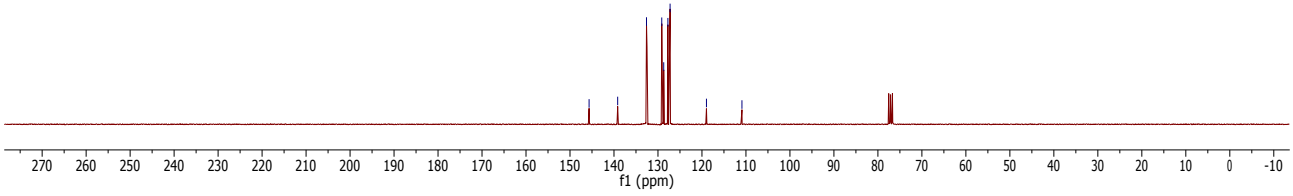

1705291326.1.fid
Kathir KM11-70
Au1H CDCl3 {C:\Bruker\TopSpin3.5pl6} 1705 26

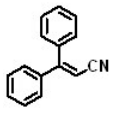

1705291326.2.fid
Kathir KM11-70
Au13C CDCl3 {C:\Bruker\TopSpin3.5pl6} 1705 26

163.15
138.94
137.10
130.50
130.09
129.61
128.72
128.61
128.53
117.98
94.95

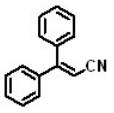

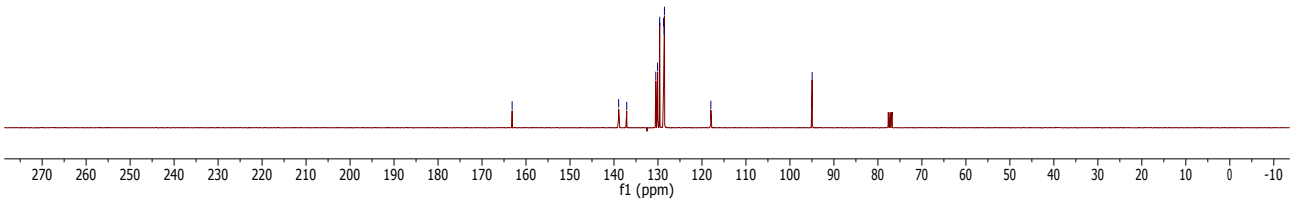

170529.328.1.fid
Kathir KM11-74
Au1H CDCl3 {C:\Bruker\TopSpin3.5pl6} 1705 28

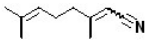

170529.328.2.fid
Kathir KM11-74
Au13C CDCl3 {C:\Bruker\TopSpin3.5pl6} 1705 28

165.13
165.02
133.32
133.20
122.21
122.16
117.28
116.98
95.80
95.22
38.57
36.28
26.13
25.65
25.62
25.60
22.90
21.03
17.72
17.66

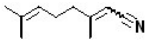

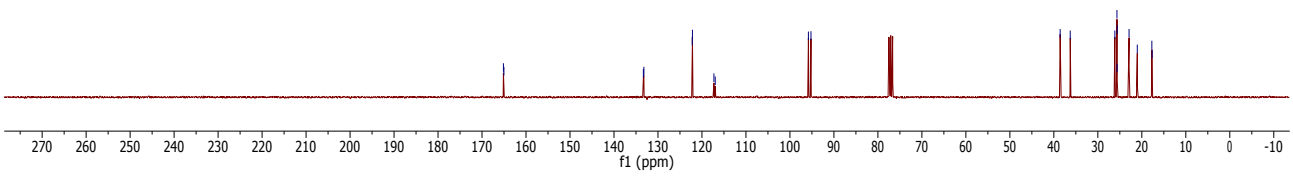

170529.329.1.fid
Kathir KM11-76
Au1H CDCl3 {C:\Bruker\TopSpin3.5pl6} 1705 29

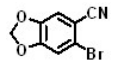

170529.329.2.fid
Kathir KM11-76
Au13C CDCl3 {C:\Bruker\TopSpin3.5pl6} 1705 29

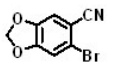

170529.330.1.fid
Kathir KM11-77
Au1H CDCl3 {C:\Bruker\TopSpin3.5pl6} 1705 30

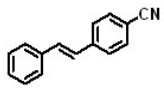

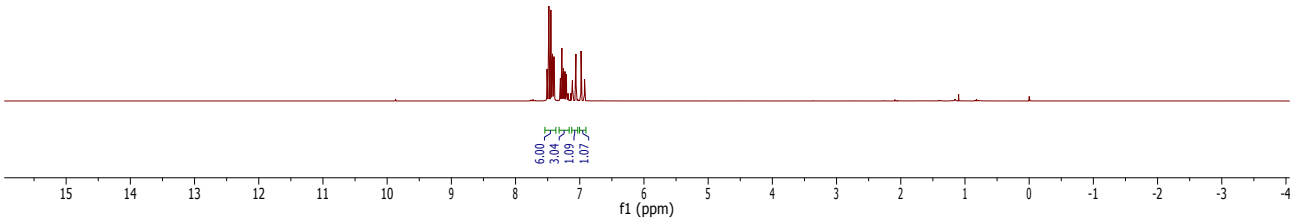

170529.330.2.fid
Kathir KM11-77
Au13C CDCl3 {C:\Bruker\TopSpin3.5pl6} 1705 30

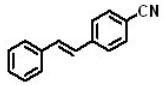

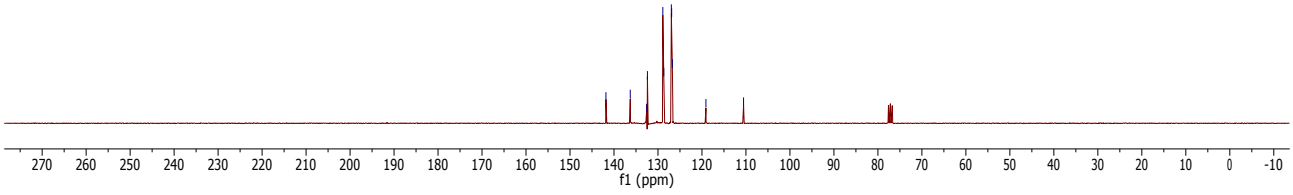

1706l3.f340.10.fid
Kathir KM11-142
PROTON CDCl3 {C:\Bruker\TopSpin3.5pl6} 1706 40

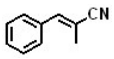

1706l3.f340.11.fid
Kathir KM11-142
C13CPD CDCl3 {C:\Bruker\TopSpin3.5pl6} 1706 40

144.43
134.12
129.35
129.32
128.71
121.29
109.68
16.82

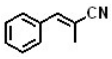

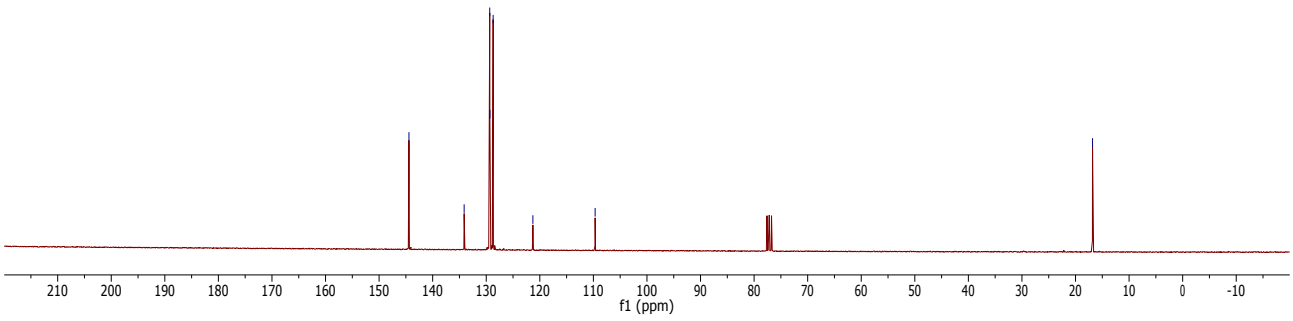

1706l3.f342.10.fid
Kathir KM11-144
PROTON CDCl3 {C:\Bruker\TopSpin3.5pl6} 1706 42

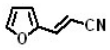

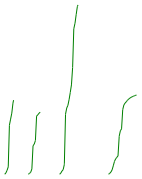

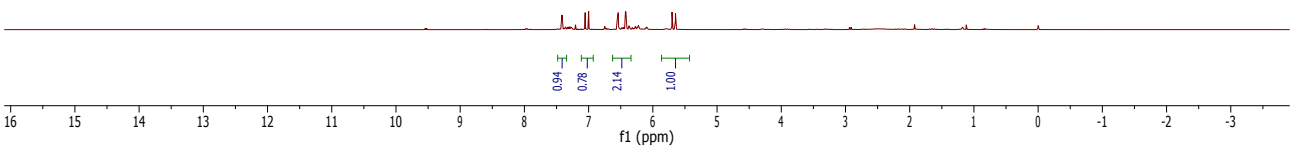

1706l3.f342.11.fid
Kathir KM11-144
C13CPD CDCl3 {C:\Bruker\TopSpin3.5pl6} 1706 42

149.79
145.47
136.15
118.28
115.47
112.64
93.34

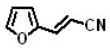

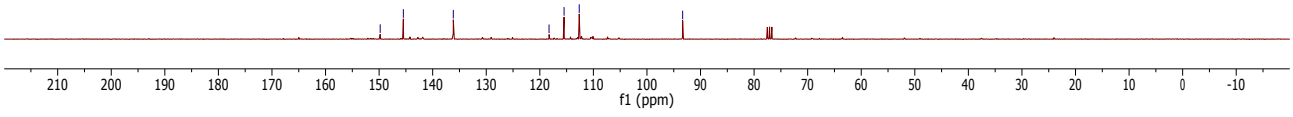

1706i3.f344.10.fid
Kathir KM11-146
PROTON CDCl3 {C:\Bruker\TopSpin3.5pl6} 1706 44

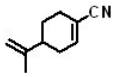

1706i3.f344.11.fid
Kathir KM11-146
C13CPD CDCl3 {C:\Bruker\TopSpin3.5pl6} 1706 44

147.72
144.62
119.53
112.06
109.84
39.20
30.96
26.93
26.28
20.63

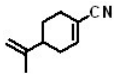

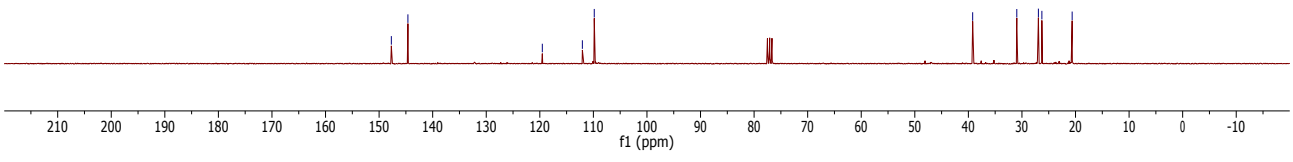

170619.f337.10.fid
Kathir KM11-148
PROTON DMSO {C:\Bruker\TopSpin3.5pl6} 1706 37

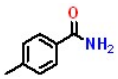

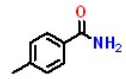

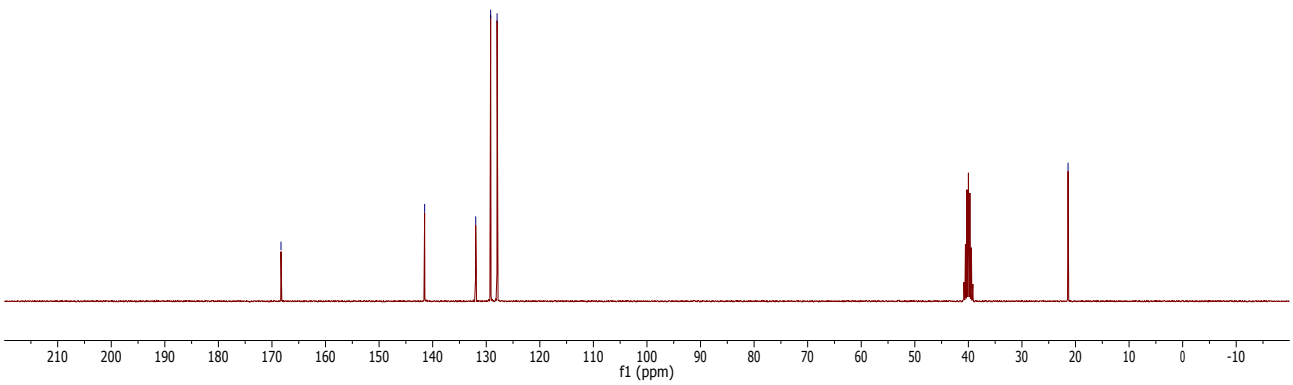

170619.f338.10.fid
Kathir KM11-162
PROTON DMSO {C:\Bruker\TopSpin3.5pl6} 1706 38

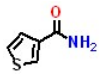

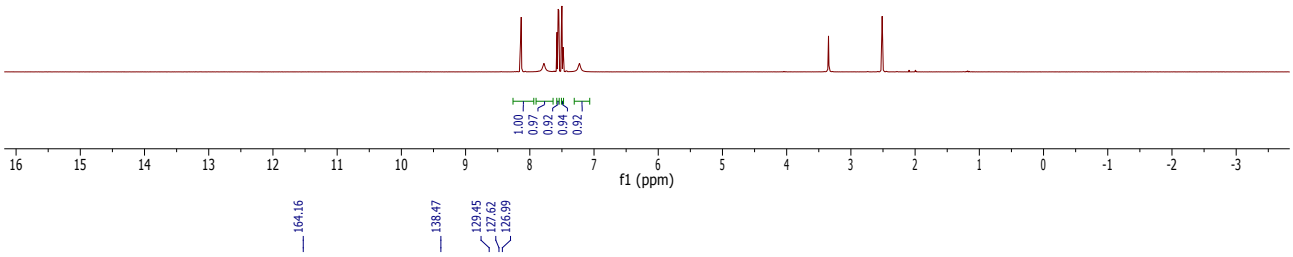

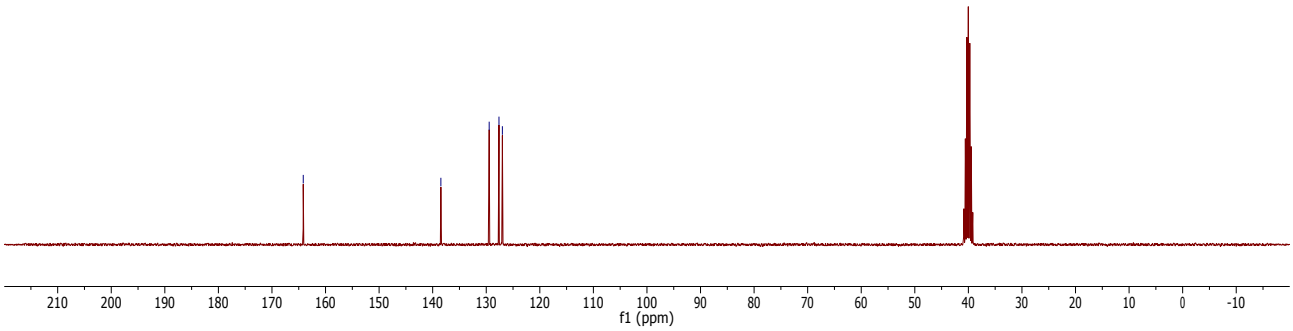

170619.f339.10.fid
Kathir KM11-190
PROTON DMSO {C:\Bruker\TopSpin3.5pl6} 1706 39

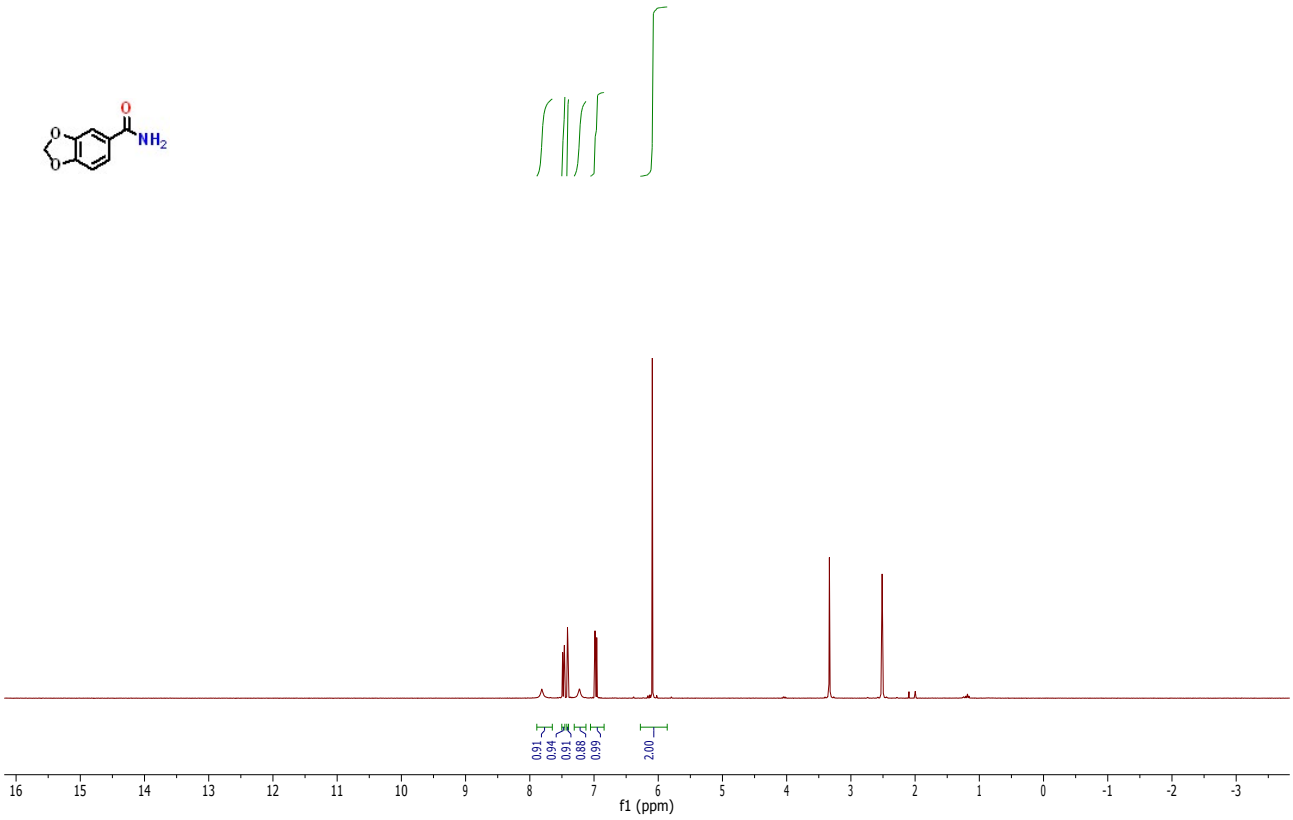

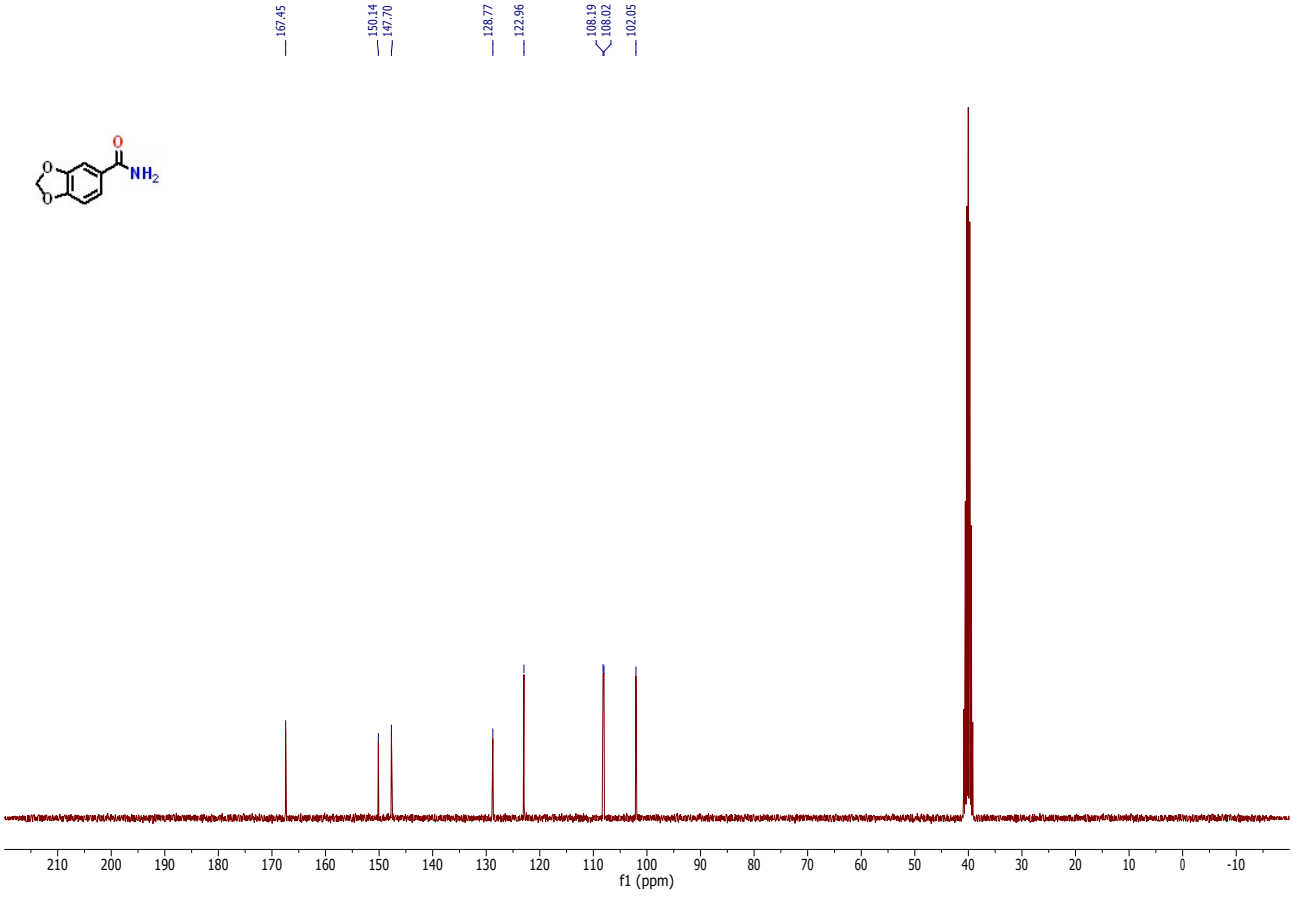

170619.f340.10.fid
Kathir KM11-196
PROTON DMSO {C:\Bruker\TopSpin3.5pl6} 1706 40

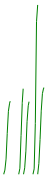

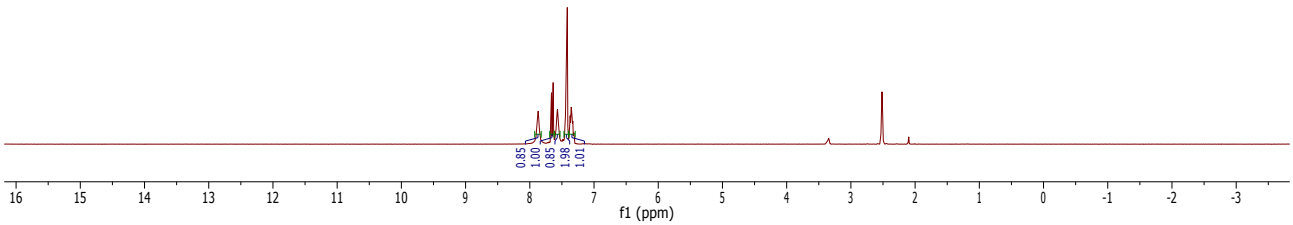

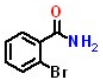

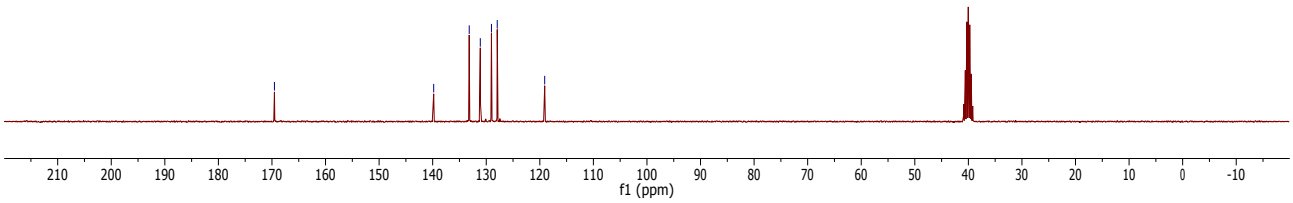

170619.f341.10.fid
Kathir KM11-197
PROTON DMSO {C:\Bruker\TopSpin3.5pl6} 1706 41

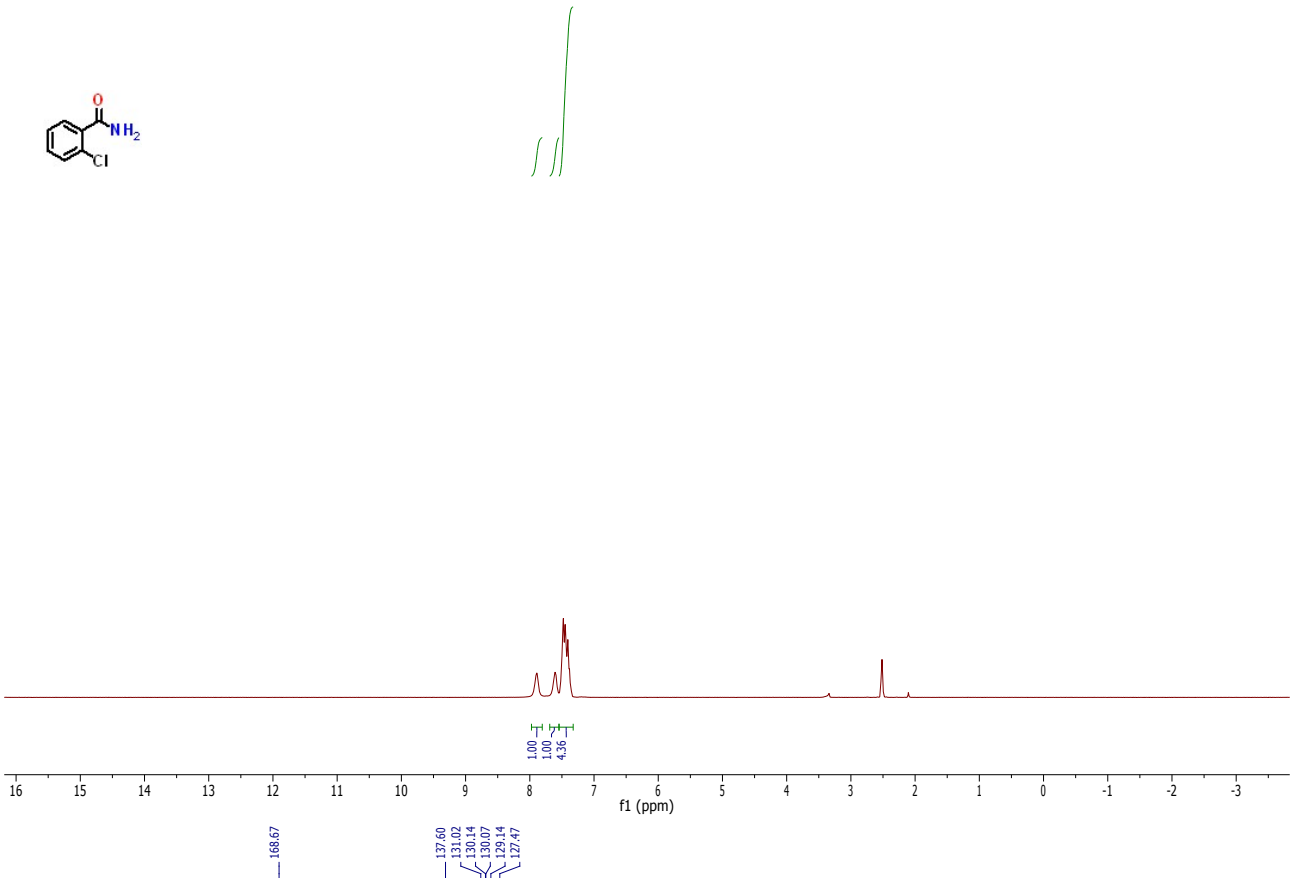

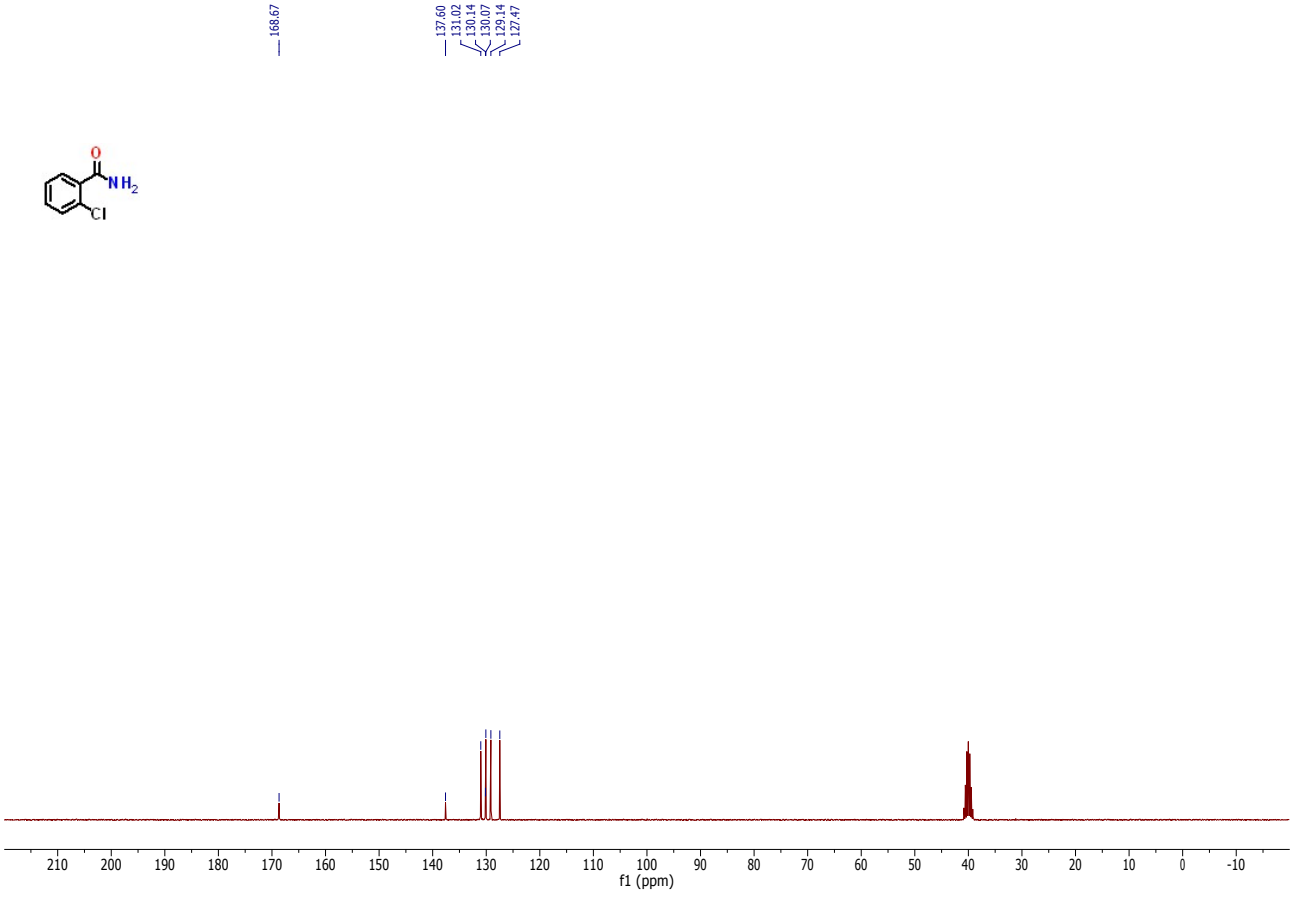

170620.f331.10.fid
Kathir KM11-198
PROTON DMSO {C:\Bruker\TopSpin3.5pl6} 1706 31

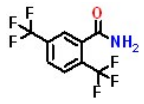

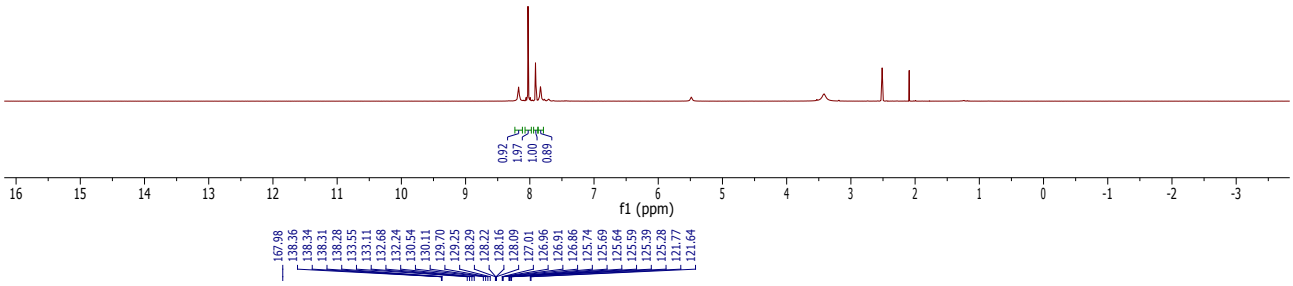

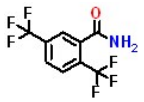

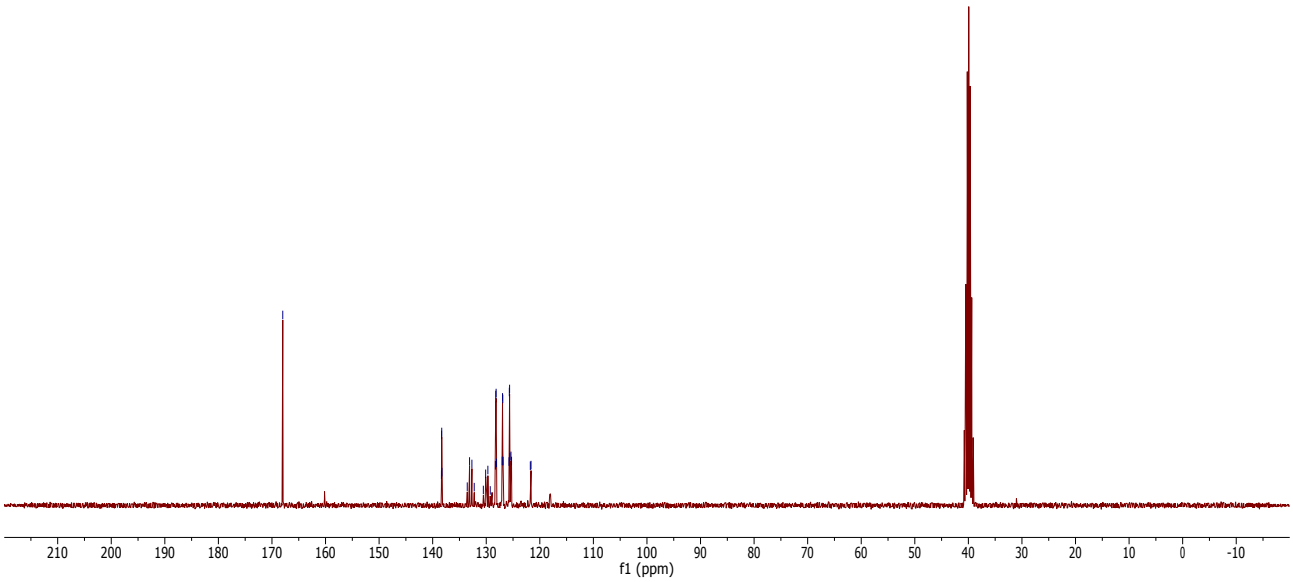

170620.f332.10.fid
Kathir KM11-199
PROTON DMSO {C:\Bruker\TopSpin3.5pl6} 1706 32

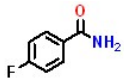

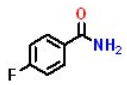

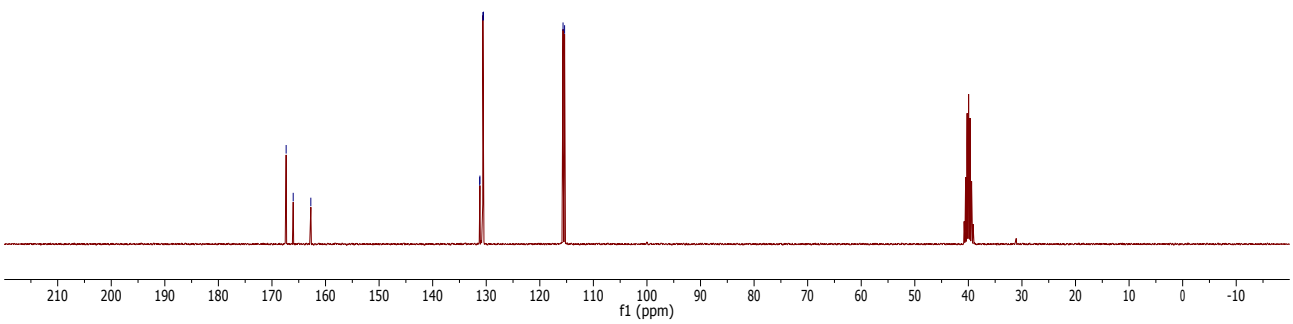

170620.f333.10.fid
Kathir KM11-202
PROTON DMSO {C:\Bruker\TopSpin3.5pl6} 1706 33

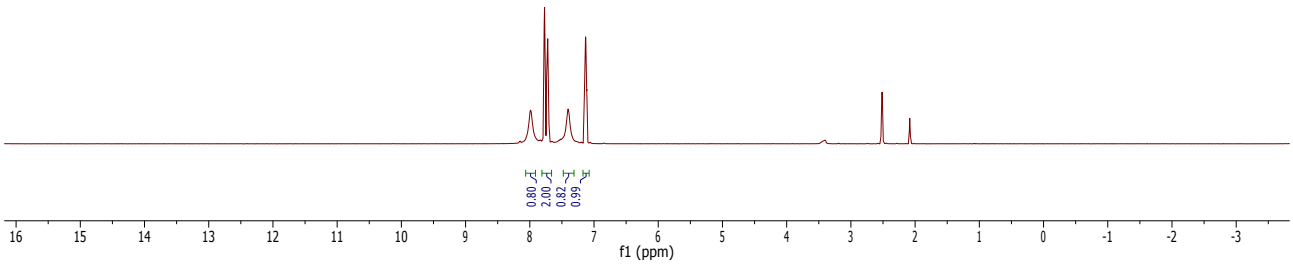

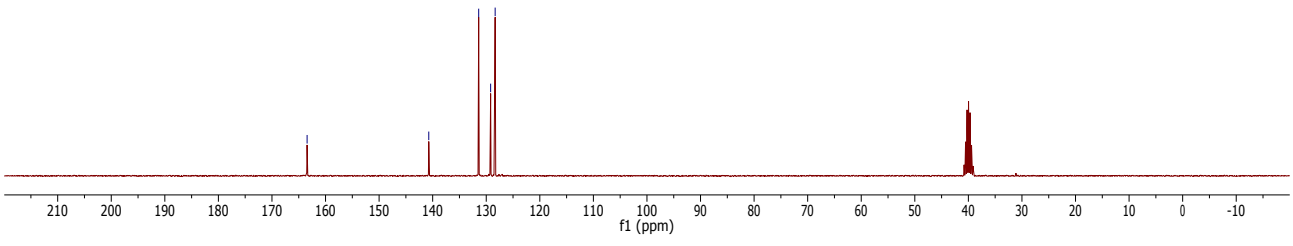

170620.f334.10.fid
Kathir KM11-205
PROTON DMSO {C:\Bruker\TopSpin3.5pl6} 1706 34

170620.f335.10.fid
Kathir KM11-214
PROTON DMSO {C:\Bruker\TopSpin3.5pl6} 1706 35

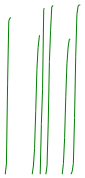

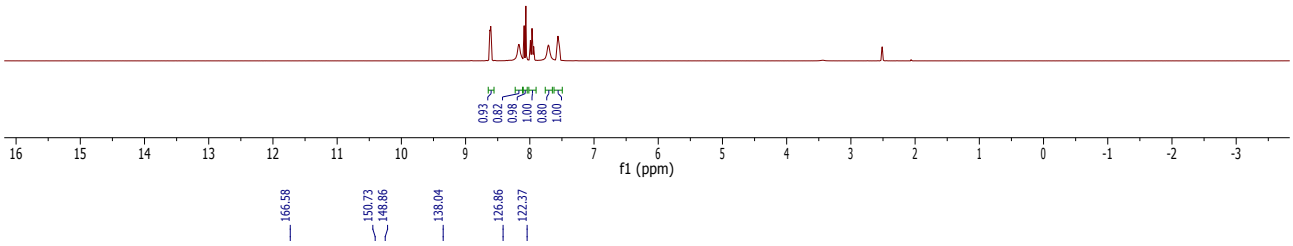

166.58
150.73
148.86
138.04
126.86
122.37

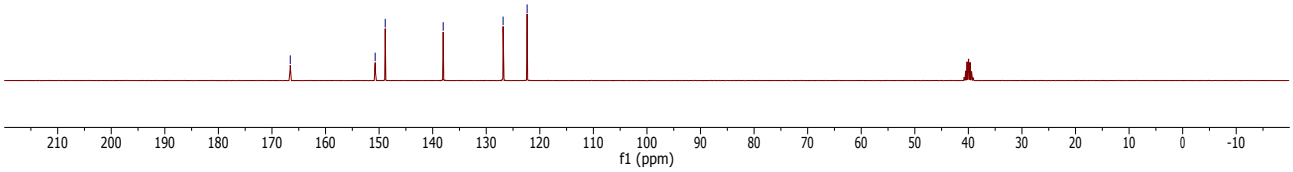

170621.f356.10.fid
Kathir/ KM II-211
PROTON DMSO {C:\Bruker\TopSpin3.5pl6} 1706 56

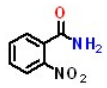

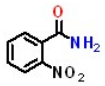

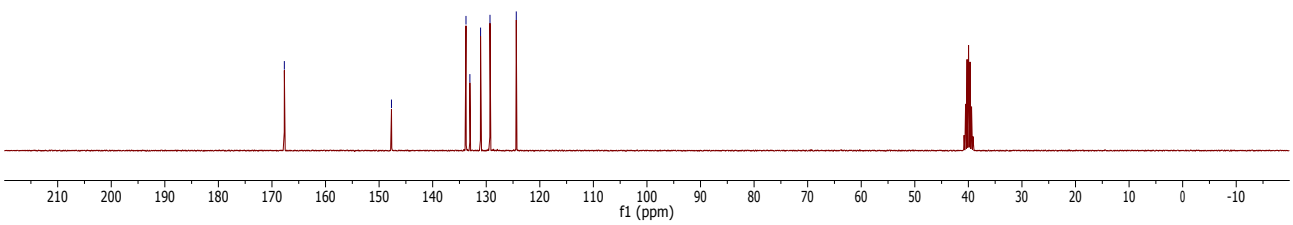

170621.f357.10.fid
Kathir/ KM II-213
PROTON DMSO {C:\Bruker\TopSpin3.5pl6} 1706 57